Smooth thin-layer asymptotic expansions for free-surface yield-stress flows

Danila Denisenko, Gael Loic Richard, Guillaume Chambon

Smooth thin-layer asymptotic expansions for free-surface yield-stress flows

Danila Denisenko*, Gaël Loïc Richard and Guillaume Chambon

[a]Univ. Grenoble Alpes, INRAE, CNRS, IRD, Grenoble INP, IGE, Grenoble, 38000, France

ARTICLE INFO

Keywords:
viscoplastic fluids
shallow flows
asymptotic expansion
asymptotic matching

ABSTRACT

We derive two asymptotic expansions with a smooth velocity field for free-surface viscoplastic flows down an inclined plane in the shallow-flow approximation. The first expansion is based on the classical Herschel-Bulkley constitutive law by using asymptotic matching at the interface between the pseudo-plug and the sheared layer. In contrast to previous works, where authors considered only one term in the transition layer, we compute two extra terms to guarantee a smooth transition of the inertial contribution from the sheared layer to the pseudo-plug. However, the terms associated to the transition layer are solutions of nonintegrable equations, thus preventing the potential use of this expansion for deriving a shallow-flow model. The second asymptotic expansion is based on an alternative tensorial extension of the Herschel-Bulkley law, for which the alignment between the yield-stress tensor and the strain-rate tensor is relaxed, while the von Mises criterion is kept. In this case, smooth asymptotic expansions of the velocity field are given by fully analytical expressions. Comparison of these two expansions with experiments shows that both give essentially equivalent and relatively good agreement.

1. Introduction

Thin-layer, or shallow-flow, approximation is largely used for simulating free-surface flows and deriving effective models of reduced dimensionality with boundary conditions directly incorporated into the equations. Since the pioneering work of Saint-Venant [1], a countless number of studies relied on this approach in hydraulics and fluid mechanics [2, 3]. Thin-layer models include lubrication models with one single evolution equation [4–6], as well as more general shallow-flow models with two [7–10] or more equations [11–14]. The aforementioned studies are mainly related to Newtonian or power-law fluids. For viscoplastic fluids, i.e., for materials that behave like a solid body as the stress remains below the yield stress and like a viscous fluid above this threshold, the number of works on thin-layer modelling is much more limited [15–19]. Yet, important applications of viscoplastic fluids in, e.g., geophysical engineering [8] or food processing [20], require developing efficient thin-layer models. In this work, we consider free-surface flows of idealized viscoplastic fluids down an inclined plane under gravity. Idealized viscoplasticity refers to a perfectly rigid behavior in the unyielded, solid-like regime.

Formally, thin-layer models can be derived from Cauchy momentum equations based on an asymptotic expansion with respect to the flow aspect ratio $\varepsilon = H/L$, where H and L denote characteristic depth and length of the flow, respectively. To properly account for the fluid rheology, the derived asymptotic models should be consistent, i.e., be equivalent to the primitive equations, at least at order $O(\varepsilon)$. Otherwise the models fail to correctly capture, e.g., the instability threshold [3, 11, 16].

For Newtonian and power-law fluids, smooth and fully analytical asymptotic expansions of the velocity field can be obtained and used to derive consistent thin-layer models [4, 9–12, 14, 21, 22]. For viscoplastic fluids, in constrast, the construction of shallow-flow expansions is not a straightforward task. At leading order with respect to ε, the solution for Bingham and Herschel–Bulkley fluids consists of a sheared layer at the base of the flow, overlaid by an unyielded plug region close to the free surface [23, 24]. Balmforth and Craster [25] extended the analysis to the first order in ε and revealed that, for the theory to be consistent, the plug layer has to be considered as a pseudo-plug, in which the strain rate is of order $O(\varepsilon)$. These authors constructed the first-order expansion in the pseudo-plug layer, while in the sheared layer the full derivation, including inertia terms, was completed later by Fernández-Nieto et al. [18] and Chambon et al. [26].

*Corresponding author (danila.denisenko@inrae.fr)
ORCID(s): 0000-0003-1293-2633 (D. Denisenko)

However, these two-layers asymptotic expansions for viscoplastic flows suffer from several drawbacks. First, the strain rate derived at $O(\varepsilon)$ diverges at the bottom of the pseudo-plug, leading to an unphysical kink in the velocity profiles. Second, the slight shearing in the pseudo-plug is solely governed by the plastic contribution to the stresses, and not by the viscous contribution. As a consequence, the consistent model based on this expansion shows a complicated structure with non-differentiable terms [18]. Furthermore, this model exhibits an unphysical destabilizing effect of plasticity at large slopes, as shown in [19]. As first proposed by Balmforth and Craster [25], and later expanded upon by Fernández-Nieto et al. [18], the first mentioned drawback can be overcome by introducing a transition layer between the pseudo-plug and the sheared layer. These authors showed how to derive the velocity profile in this transition layer in the case of Bingham fluids. However, the extra term is given by a nonintegrable equation, thus preventing from deriving fully analytical models.

An alternative approach to eliminate the mentioned drawbacks of the asymptotic expansion for Bingham fluids was proposed in our recent paper [19]. The main idea of this approach is to remove the assumption of alignment between the yield-stress and strain-rate tensors in the constitutive law. It is then possible to construct a smooth and fully-analytical asymptotic expansion of the velocity field based on two layers only. Furthermore, the slight shearing in the pseudo-plug is governed by the viscous stress contribution, such that the mathematical structure of the expansion remains similar to that obtained for Newtonian or power-law fluids. The thin-layer model derived based on this expansion has a well-posed mathematical structure and exhibits a stabilizing effect of plasticity [19].

The main objective of this paper is to extend the two mentioned approaches to derive smooth velocity field expansions for Herschel-Bulkley fluids. For the first approach relying on the "classical" tensorial form of the constitutive law, we expand on the idea of introducing a transition layer to avoid the divergence of the strain rate at the interface between the pseudo-plug and the sheared layer. However, unlike the previous works, we construct the complete the velocity expansions and show that additional terms are actually required to ensure proper asymptotic matching with the sheared layer when inertial contribution is taken into account. The number of extra-terms required happens to depend on the rheological flow index. As in previous studies, however, these extra-terms associated with the transition layer are given by nonintegrable equations. We also extend the approach of Denisenko et al. [19] based on an alternative form of the constitutive law, in which we remove the assumption of alignment between the yield-stress and strain-rate tensor. For Herschel-Bulkley fluids, however, additional complexity is introduced by the non-linearity associated to the power-law exponent. This leads us to introduce a specific regularization of the viscous-stress tensor at $O(\varepsilon)$. Such formulation allows us to derive an analytical asymptotic expansion with a smooth velocity field. As second objective of the study is then to compare the velocity profiles provided by the two expansions to experimental data measured in free-surface viscoplastic surges [26].

The structure of the paper is the following: In §2 we present the classical tensorial formulation of Herschel–Bulkley constitutive law as well as the alternative version, and formulate the equations of the problem. In §3, we construct the shallow-flow asymptotic solution based on the introduction of a transition layer. In §4, the shallow-flow expansion for the alternative tensorial formulation of the Herschel–Bulkley law is derived. In §5, the two expansions are compared with experiments. Lastly, conclusive discussions and remarks are provided in §6.

2. Statement of the problem

Let us consider a two-dimensional gravity-driven flow of a viscoplastic fluid down an inclined plane forming an angle θ to the horizontal (Figure 1). The acceleration due to gravity is denoted by $\boldsymbol{g}$. The x-axis is parallel to the plane, while the z-axis is orthogonal to the base. The components of the velocity are denoted by u and w in the Ox and Oz-directions, respectively, and the components of the strain-rate tensor $\dot{\boldsymbol{\gamma}}$ are defined as: $\dot{\gamma}_{xx} = 2\partial_x u$, $\dot{\gamma}_{xz} = \partial_z u + \partial_x w$, $\dot{\gamma}_{zz} = 2\partial_z w$. The fluid depth is denoted by $h(x,t)$. Lastly, the fluid is assumed to be incompressible ($\mathrm{tr}\,\dot{\boldsymbol{\gamma}} = 0$) with a density ρ.

2.1. Constitutive law

The fluid is assumed to obey the Herschel–Bulkley constitutive law written as follows:

$$\tau_{ij} = \tau_{ij}^{Y} + K\dot{\gamma}_{ij}|\dot{\boldsymbol{\gamma}}|^{n-1} \qquad |\boldsymbol{\tau}| > \tau_c, \tag{2.1}$$

$$\dot{\gamma}_{ij} = 0 \qquad |\boldsymbol{\tau}| \leqslant \tau_c. \tag{2.2}$$

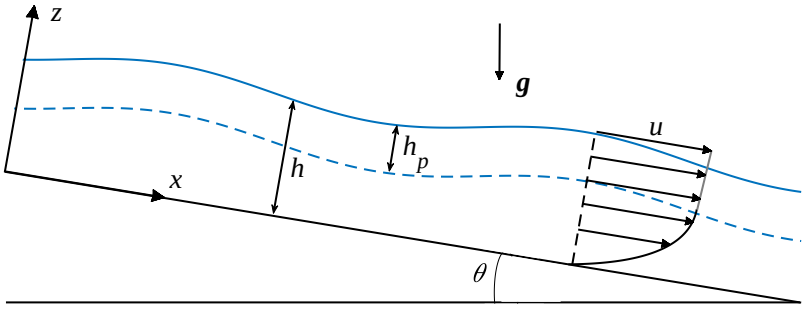

Figure 1: Definition sketch

Here $\boldsymbol{\tau} = \boldsymbol{\sigma} + \boldsymbol{I}p$ is the extra-stress tensor (with the total stress $\boldsymbol{\sigma}$ and the pressure p), and $\boldsymbol{\tau}^Y$ denotes the *yield-stress* tensor. The rheological parameters τ_c, K and n correspond to the yield stress, the consistency and the flow index of the material, respectively. The norm is defined as $|\boldsymbol{T}| = (0.5\boldsymbol{T}_{ij}\boldsymbol{T}_{ij})^{0.5}$ for any second-order tensor.

In most studies pertaining to idealized viscoplastic fluids [20, 25, 27], the yield-stress tensor $\boldsymbol{\tau}^Y$ is assumed to be aligned with the strain-rate tensor $\dot{\boldsymbol{\gamma}}$, such that:

$$\boldsymbol{\tau}^Y = \tau_c \frac{\dot{\boldsymbol{\gamma}}}{|\dot{\boldsymbol{\gamma}}|}. \tag{2.3}$$

This classical expression was first proposed by Hohenemser and Prager [28] to extend the simple-shear scalar Bingham constitutive law to a tensorial form. Later, Oldroyd [29] used this same expression of the yield-stress tensor to extend the Herschel–Bulkley law. As already mentioned, shallow-flow asymptotic expansions based on expression (2.3) are characterized by a non-smooth velocity profile at order $O(\epsilon)$, with a diverging strain rate at the base of the pseudo-plug [18, 25, 26]. The origin of this behaviour can be traced back to the singularity of the effective viscosity associated to the yield-stress tensor in Eq. (2.3), namely $\tau_c/|\dot{\boldsymbol{\gamma}}|$, when $|\dot{\boldsymbol{\gamma}}|$ goes to 0 (see §3).

As shown in our previous work for Bingham fluids [19], an effective way to suppress the above-mentioned singularity is to remove the assumption of codirectionality between the yield-stress and strain-rate tensors. In place of Eq. (2.3), we then assume that the yield-stress tensor $\boldsymbol{\tau}^Y$ satisfies the following conditions:

- The norm of $\boldsymbol{\tau}^Y$ is equal to the yield stress τ_c in yielded regions: $|\boldsymbol{\tau}^Y| = \tau_c$ for $|\dot{\boldsymbol{\gamma}}| > 0$. This condition is necessary to recover the von Mises yielding criterion.
- The trace of $\boldsymbol{\tau}^Y$ is zero in accordance with the incompressibility hypothesis: $\mathrm{tr}\,\boldsymbol{\tau}^Y = 0$.
- Normal stress differences are null in simple-shear (hence $\boldsymbol{\tau}^Y$ happens to be aligned with $\dot{\boldsymbol{\gamma}}/|\dot{\boldsymbol{\gamma}}|$ in the particular case of simple shear flows). Although clearly questionable for real fluids, this assumption is made to obtain the same leading-order solution as in models based on the classical formulation.
- The existence of a normal stress difference in the pseudo-plug at leading order, and all terms originating from these normal stresses in the asymptotic expansions, are attributed to the yield-stress tensor and not to the viscous-stress tensor. All other terms in the asymptotic expansions are attributed to the viscous-stress tensor.

As shown below (§4), these assumptions are sufficient to work out asymptotic expansion up to the first order in ϵ. Obviously, to compute flows in general cases, a complete specification of the yield-stress tensor would be required. However, since our goal here is to derive tractable shallow-flow asymptotic solutions, we shall limit ourselves to these assumptions in the frame of this paper. The constitutive law (2.1) together with the four conditions introduced above can be considered as an alternative tensorial extension of the Herschel–Bulkley law, since the classical scalar expression $\tau = \tau_c + |\dot{\gamma}|^n$ is recovered in simple-shear flows. Removing the codirectionality between the yield-stress and strain-rate tensors can be seen as a specific regularization, in that it avoids the singularity of the effective viscosity associated to the yield-stress tensor in (2.3). However, unlike with classical regularization approaches [20, 30], in which the solid behaviour is replaced by a highly viscous fluid, the material here remains truly rigid below the yield point.

Hereinafter, for $|\boldsymbol{\tau}| > \tau_c$, we split the extra-stress tensor in its yield-stress and viscous contributions respectively:

$$\tau_{ij} = \tau^Y_{ij} + \tau^v_{ij}, \quad \tau^v_{ij} = K\dot{\gamma}_{ij}|\dot{\boldsymbol{\gamma}}|^{n-1}. \tag{2.4}$$

Compared to the Bingham case, with $n < 1$, an additional complexity arises from the divergence of the effective viscosity associated to the viscous stress tensor, namely $K|\dot{\boldsymbol{\gamma}}|^{n-1}$, when $|\dot{\boldsymbol{\gamma}}|$ approaches 0. As a consequence, a specific regularization of the power-law viscous-stress tensor at $O(\varepsilon)$ will also need to be introduced for deriving expansions based on the alternative formulation of the constitutive law (see §4 for more details).

2.2. Governing equations

The fluid motion is governed by the mass and momentum conservation equations, completed by kinematic and dynamic boundary conditions on the bottom wall and at the free surface. The continuity equation reads

$$\partial_x u + \partial_z w = 0. \tag{2.5}$$

The Cauchy momentum balances in the Ox and Oz directions are

$$\rho\left(\partial_t u + u\partial_x u + w\partial_z u\right) = -\partial_x p + \rho g \sin\theta + \partial_z \tau_{xz} + \partial_x \tau_{xx}, \tag{2.6}$$

$$\rho\left(\partial_t w + u\partial_x w + w\partial_z w\right) = -\partial_z p - \rho g \cos\theta + \partial_x \tau_{xz} + \partial_z \tau_{zz}. \tag{2.7}$$

At the bottom $z = 0$, the no-penetration and the no-slip conditions read

$$u_{|_{z=0}} = w_{|_{z=0}} = 0. \tag{2.8}$$

At the free surface $z = h(x)$, the kinematic boundary condition reads

$$\partial_t h + u_{|_{z=h(x)}} \partial_x h = w_{|_{z=h(x)}}, \tag{2.9}$$

and the dynamic boundary conditions are

$$\left[1 - \left(\partial_x h\right)^2\right] \tau_{xz|_{z=h(x)}} = 2(\partial_x h)\tau_{xx|_{z=h(x)}}, \tag{2.10}$$

$$\left[1 - \left(\partial_x h\right)^2\right] p_{|_{z=h(x)}} = -\left[1 + \left(\partial_x h\right)^2\right] \tau_{xx|_{z=h(x)}}. \tag{2.11}$$

Note that capillary effects are neglected here, and the atmospheric pressure is constant and taken equal to zero.

2.3. Shallow-flow scaling

Let a H and L be characteristic dimensions of the flow in the Oz and Ox direction, respectively, and U be a characteristic velocity in the Ox direction. The shallow-flow hypothesis assumes that the aspect ratio $\varepsilon = H/L$ is small. For viscoplastic fluids, the main dimensionless groups of the problem are the Reynolds number Re, the Froude number Fr, and the Bingham number Bi, defined as:

$$Re = \frac{\rho U^{2-n} H^n}{K}, \qquad Fr = \frac{U}{\sqrt{gH\cos\theta}}, \qquad Bi = \frac{\tau_c}{K}\left(\frac{H}{U}\right)^n.$$

These numbers and the slope angle θ are all assumed to be of order $O(1)$ with respect to aspect ratio ε. To reformulate the problem (2.5)-(2.11) into a dimensionless form, let us express the variables of the problem as:

$$x = Lx'; \quad z = Hz'; \quad u = Uu'; \quad w = \varepsilon U w'; \quad t = \frac{L}{U}t'; \quad h = Uh';$$

$$p = \rho g H \cos\theta p'; \quad \tau_{ij} = \tau_c \tau'_{ij}; \quad |\boldsymbol{\tau}| = \tau_c |\boldsymbol{\tau}'|; \quad |\dot{\boldsymbol{\gamma}}| = \frac{U}{H}|\dot{\boldsymbol{\gamma}}'|.$$

For convenience, we omit the primes in what follows. The continuity equation (2.5) keeps the form

$$\partial_x u + \partial_z w = 0, \tag{2.12}$$

while the scaled momentum equations (2.6)-(2.7) take the following form

$$\varepsilon\left(\partial_t u + u\partial_x u + w\partial_z u\right) = -\frac{\varepsilon}{Fr^2}\partial_x p + \frac{\lambda}{Re} + \frac{Bi}{Re}\partial_z \tau_{xz} + \frac{\varepsilon Bi}{Re}\partial_x \tau_{xx}, \tag{2.13}$$

$$\varepsilon^2\left(\partial_t w + u\partial_x w + w\partial_z w\right) = -\frac{1}{Fr^2}\left(1 + \partial_z p\right) + \frac{\varepsilon Bi}{Re}\partial_x \tau_{xz} + \frac{Bi}{Re}\partial_z \tau_{zz}, \tag{2.14}$$

with the driving parameter λ given by

$$\lambda = \frac{\rho g H^2 \sin\theta}{KU} = \frac{Re}{Fr^2}\tan\theta.$$

In the scaled variables, the yielding criterion reduces to $|\boldsymbol{\tau}| = 1$. Then, for $|\boldsymbol{\tau}| > 1$, the expressions for the viscous and yield-stress components of (2.4) are transformed to

$$\tau_{xx} = \tau_{xx}^Y + \tau_{xx}^v, \qquad \tau_{xx}^v = \frac{2\varepsilon}{Bi}\partial_x u |\dot{\boldsymbol{\gamma}}|^{n-1}, \tag{2.15}$$

$$\tau_{xz} = \tau_{xz}^Y + \tau_{xz}^v, \qquad \tau_{xz}^v = \frac{1}{Bi}\left(\partial_z u + \varepsilon^2 \partial_x w\right)|\dot{\boldsymbol{\gamma}}|^{n-1}. \tag{2.16}$$

The condition on the norm of the dimensionless yield-stress tensor is

$$\left(\tau_{xx}^Y\right)^2 + \left(\tau_{xz}^Y\right)^2 = 1. \tag{2.17}$$

The no-penetration and the no-slip conditions (2.8) take the same form

$$u_{|_{z=0}} = w_{|_{z=0}} = 0, \tag{2.18}$$

while the scaled kinematic and dynamic boundary conditions (2.9)-(2.11) are rewritten as

$$\partial_t h + u_{|_{z=h(x)}}\partial_x h = w_{|_{z=h(x)}}, \tag{2.19}$$

$$\left[1 - \varepsilon^2\left(\partial_x h\right)^2\right]\tau_{xz}|_{z=h(x)} = 2\varepsilon(\partial_x h)\tau_{xx}|_{z=h(x)}, \tag{2.20}$$

$$\left[1 - \varepsilon^2\left(\partial_x h\right)^2\right] p_{|_{z=h(x)}} = -\frac{Bi Fr^2}{Re}\left[1 + \varepsilon^2\left(\partial_x h\right)^2\right]\tau_{xx}|_{z=h(x)}. \tag{2.21}$$

Lastly, the norms of the dimensionless stress and the strain-rate tensors read

$$|\boldsymbol{\tau}| = \sqrt{\tau_{xx}^2 + \tau_{xz}^2} \qquad |\dot{\boldsymbol{\gamma}}| = \sqrt{\left(\partial_z u + \varepsilon^2\partial_x w\right)^2 + 4\varepsilon^2\left(\partial_x u\right)^2}. \tag{2.22}$$

2.4. Shallow-flow asymptotic expansions

In the following sections, we derive shallow-flow asymptotic solutions of Eqs. (2.12)–(2.22) for $\varepsilon \ll 1$. Let us thus assume the existence of regular expansions in the form

$$f = f^{(0)} + \varepsilon f^{(1)} + \ldots \tag{2.23}$$

for all variables of the problem, namely longitudinal and normal velocities u and w, pressure p and stress tensor components τ_{ij}.

As mentioned in introduction, the structure of thin viscoplastic flows generally consists of a pseudo-plug, in which the strain rate vanishes at leading order, overlying a sheared layer [25]. These two layers are separated by a so-called fake yield surface. Two strategies are followed to obtain smooth asymptotic solutions at first order in ε. In §3, expansions are derived based on the classical formulation of the constitutive law (see §2.1). In this case, a third, transition layer has to be introduced to ensure asymptotic matching between the pseudo-plug and the sheared layer and avoid the divergence of the strain rate at the fake yield surface. In §4, we use instead the alternative formulation of the constitutive law proposed in 2.1. In this case, the strain rate remains bounded in the pseudo-plug at $O(\varepsilon)$ and no asymptotic matching is required.

3. Asymptotic expansion: "classical" approach

We first recall the non-smooth solutions that are obtained when considering the classical expression of the yield-stress tensor (2.3) and a simple matching at the fake yield surface. Smooth solutions based on proper asymptotic matching are then explicitly constructed.

3.1. Simple matching

The derivation of the asymptotic expansion at first-order in ε closely follows the work of Chambon et al. [26]. However, unlike this former study, which considered a small slope angle θ, we consider here that $\theta = O(1)$. Accordingly, the pressure gradient term only contributes to the longitudinal momentum (2.13) balance at $O(\varepsilon)$, and not at leading order. Complete calculations are presented in Appendix A. We only recall here the final expressions for the longitudinal velocity at leading and first order, $u^{(0)}$ and $u^{(1)}$.

The leading-order longitudinal velocity $u^{(0)}$ is given by

$$u^{(0)} = \frac{n\lambda^{\frac{1}{n}}}{n+1} \begin{cases} (h-h_p)^{\frac{n+1}{n}} - (h-h_p-z)^{\frac{n+1}{n}} & z < h-h_p, \\ (h-h_p)^{\frac{n+1}{n}} & z \geqslant h-h_p, \end{cases} \tag{3.1}$$

where the constant $h_p = Bi/\lambda$ denotes the thickness of the pseudo-plug. As clear from expression (3.1), the leading-order strain rate $|\dot{\boldsymbol{\gamma}}|^{(0)} = \partial_z u^{(0)}$ vanishes for $z > h - h_p$, indicating a pseudo-plug layer. Note that the constant pseudo-plug thickness is obtained here in the framework of the asymptotic expansion with $\theta = O(1)$. In contrast, in [26], the pseudo-plug thickness was found to vary along the flow due to the contribution of the pressure term at leading order. Regardless of this difference, as the pressure term is accounted for at $O(\varepsilon)$ in the present approach, we do not expect to have significant differences between the two approaches for shear rates and velocities calculated at first order. Furthermore, the variations of pseudo-plug thickness in the former approach led to terms involving the second-order derivative $\partial_{xx} h$ in the expansions at $O(\varepsilon)$, significantly complicating the expressions.

The expression for the first-order velocity correction $u^{(1)}$ reads

$$u^{(1)} = \begin{cases} \dfrac{1}{n}\lambda^{\frac{1-n}{n}} \displaystyle\int_0^z (h-h_p-\zeta)^{\frac{1-n}{n}} \Big[\mathcal{I}(\zeta) + \mathcal{P}(\zeta)\Big] d\zeta & z < h-h_p, \\ 2h_p \sqrt{1-\left(\dfrac{h-y}{h_p}\right)^2} \left|\partial_x u^{(0)}_{pl}\right| + u^{(1)}_{sh}{}_{|z=h-h_p} & z \geqslant h-h_p, \end{cases} \tag{3.2}$$

where $u^{(1)}_{sh}$ denotes the expression of $u^{(1)}$ in the sheared layer, and the inertial $\mathcal{I}$ and pressure $\mathcal{P}$ contributions are given by

$$\mathcal{I}(z) = -Re \int_z^h \Big(\partial_t u^{(0)} + u^{(0)}\partial_x u^{(0)} + w^{(0)}\partial_z u^{(0)}\Big), \quad \mathcal{P} = \frac{Re}{Fr^2}(z-h)\partial_x h. \tag{3.3}$$

The functions (3.1) and (3.2) are continuous everywhere in the flow domain and can formally be used to compute the velocity field at the first order in ε. However, the expressions for the derivative $\partial_z u^{(1)}$ read

$$\partial_z u^{(1)} = \begin{cases} \dfrac{1}{n}\lambda^{\frac{1-n}{n}} \left(h-h_p-z\right)^{\frac{1-n}{n}} \Big[\mathcal{I}(z) + \mathcal{P}(z)\Big] & z < h-h_p, \\ \dfrac{2(h-z)/h_p}{\sqrt{1-((h-z)/h_p)^2}} \left|\partial_x u^{(0)}\right| & z \geqslant h-h_p. \end{cases} \tag{3.4}$$

and feature a discontinuity at $z = h - h_p$. Namely, the derivative $\partial_z u$ in the pseudo-plug diverges for $z \to h - h_p$, while the expression in the sheared layer vanishes:

$$\lim_{z \to (h-h_p)^-} \partial_z u^{(1)} = 0, \tag{3.5}$$

$$\lim_{z\to(h-h_p)^+} \partial_z u^{(1)} = \infty. \tag{3.6}$$

As a result, the velocity profile presents a nonphysical kink at the fake yield surface [26]. Note that the divergence of the strain rate for $z \to (h - h_p)^+$ also appears in contradiction with the very definition of the pseudo-plug, in which $|\dot{\boldsymbol{\gamma}}|$ should remain $O(\varepsilon)$.

3.2. Asymptotic matching

The above contradiction comes from the direct matching of the two the asymptotic expansions at the fake yield-surface in (3.2), via the term $u^{(1)}_{sh\,|z=h-h_p}$. A proper way to overcome this issue is to consider instead an asymptotic matching, through the introduction of a third transition layer located between the sheared layer and the pseudo-plug. This approach has already been proposed for Bingham fluids by Balmforth and Craster [25]. However, these authors postulated an incorrect thickness for the transition layer. This issue was later corrected by Fernández-Nieto et al. [18]. None of these studies, however, went on to construct the complete velocity profiles. We extend here the approach of [18] for Herschel–Bulkley fluids, and show that additional complexities arise to ensure proper matching between the sheared and the transition layers.

As proposed by Fernández-Nieto et al. [18] for Bingham fluids, let us thus consider a transition layer with thickness of order $O(\varepsilon^\kappa)$, $\kappa > 0$, in which the velocity is expressed as:

$$u = u^{(0)}_{pl}(x,t) + \varepsilon^{\alpha+\kappa} U_{tr}(x,\xi,t) + \dots \tag{3.7}$$

where $0 < \alpha < 1$ and the zoomed-in variable ξ is given by

$$\xi = \frac{z-(h-h_p)}{\varepsilon^\kappa}. \tag{3.8}$$

The function $u^{(0)}_{pl}$ corresponds to the leading-order velocity for the pseudo-plug given by (3.1).

From (3.7), the expansion for the velocity derivative reads

$$\partial_z u = \varepsilon^\alpha S(x,\xi,t) + \dots \tag{3.9}$$

where S is the derivative of U_{tr} with respect to ξ. From (2.16), the shear stress in the transition layer can thus be expanded as

$$\tau_{xz} = \frac{\varepsilon^\alpha S}{\sqrt{\varepsilon^{2\alpha} S^2 + 4\varepsilon^2 \left(\partial_x u^{(0)}_{pl}\right)^2}} + \frac{\varepsilon^{n\alpha}}{Bi} S^n + \dots \tag{3.10}$$

and momentum balance then leads to the following equation at lowest order:

$$-\frac{\lambda}{Bi}\varepsilon^\kappa \xi = -2\varepsilon^{2(1-\alpha)} \frac{1}{S^2}\left(\partial_x u^{(0)}_{pl}\right)^2 + \frac{\varepsilon^{n\alpha}}{Bi} S^n. \tag{3.11}$$

Balancing terms in (3.11) requires $2(1-\alpha) = n\alpha = \kappa$, i.e.,

$$\alpha = \frac{2}{(2+n)}, \qquad \kappa = \frac{2n}{(2+n)}, \tag{3.12}$$

and the following equation for $S(\xi)$ is obtained:

$$S^n + \lambda\xi = 2\frac{Bi}{S^2}\left(\partial_x u^{(0)}_{pl}\right)^2. \tag{3.13}$$

The above equation cannot be solved analytically if $n < 1$, so that a numerical implementation is required. Moreover, note that the inertial and pressure terms do not contribute to this expression for S. Accordingly, the expansion

(3.9) cannot be matched at first-order with the expression (3.4) for $\partial_z u$ in the sheared layer. This difficulty, which was not anticipated in [18], implies that the one-term expansion (3.7) assumed in the transition layer is not sufficient. Additional terms need to be included. Moreover, as explained in Appendix B, the number of these additional terms depends on the value of n.

The complete derivation of the transition layer expressions is lengthy and presented in Appendix (B). We consider specifically the case $2/5 \leqslant n < 2/3$, for which two additional terms need to be introduced in the expansions (3.7) and (3.9). These terms are determined similarly as for the function $S(\xi)$ above, and it can be shown that the expansion in the transition layer is then properly matched at first order with the expansions obtained in both the sheared layer and in the pseudo-plug. A final solution valid over the whole fluid domain can then be constructed as a composite approximation combining the expansion in the transition layer (inner solution) and the expansions in the sheared layer and pseudo-plug (outer solution). This leads to the following expression for the longitudinal velocity:

$$u = u^{(0)}(z) + \varepsilon u^{(1)}(z) + \varepsilon^{\frac{2(n+1)}{n+2}}\,[C(z) - C(0)] + \varepsilon^{\frac{2(2n+1)}{n+2}}\,[T(z) - T(0)] + \varepsilon^{\frac{4+n}{n+2}}\Big[\mathcal{I}(h-h_p) + \mathcal{P}(h-h_p)\Big]\,[D(z) - D(0)] \quad (3.14)$$

The first two terms correspond to the leading-order solution (3.1) and the first order correction (3.2). The functions C, T and D come from the transition layer and are defined in Appendix B.

The extra-terms associated to the transition layer in (3.14) are significant only in a neighborhood of thickness $O(\varepsilon^\kappa)$ from the fake yield surface. Note that, formally, these terms are all smaller than $O(\varepsilon)$. For the derivative $\partial_z u$, however, the term associated to the function C is intermediate between $O(1)$ and $O(\varepsilon)$. Furthermore, it can be shown that $\varepsilon\partial_z u^{(1)} \sim -\varepsilon^{2(n+1)/(n+2)}\partial_z C$ as $z \to h - h_p$, such that this term effectively compensates the divergence of the strain rate at the fake yield surface. Although the two terms associated to the functions D and T lead to contributions that are formally smaller than $O(\varepsilon)$ in the expression of $\partial_z u$ (see Appendix B), these terms are nevertheless essential to construct a smooth velocity profile at first order. Indeed, $\varepsilon^{(4+n)/(n+2)}\partial_z D$ becomes $O(\varepsilon)$ as $z \to h - h_p$, and this term is required to match the inertial and pressure terms at first order in the sheared layer. The term in T is required to satisfy the constitutive law (2.16) close to the fake yield surface when $2/5 \leqslant n < 2/3$. This term can however be neglected in the case $n \geqslant 2/3$.

The expansion (3.14) provides a velocity field with a smooth transition at the fake-yield surface. The functions C, T and D, however, cannot be expressed analytically and have to be computed numerically. Velocity profiles computed from (3.14) will be shown and compared to experimental data in §5.

4. Asymptotic expansion: alternative approach

As demonstrated in the previous section, the derivation of smooth velocity expansions based on the classical expression of the yield-stress tensor (2.3) requires asymptotic matching at the fake yield surface and leads to a nonlinear equation (3.13) that cannot be solved analytically. We show here that, by relaxing the condition (2.3) on the alignment of the yield-stress and strain-rate tensors, an alternative, fully analytical shallow-flow expansion with a smooth velocity field can be derived for Herschel-Bulkley fluids. Recall that the yield-stress tensor is assumed to satisfy the four conditions formulated in §2.1. The specific case of Bingham fluids ($n = 1$) has already been addressed in our previous paper [19]. However, as explained below, additional difficulties arise when considering the case $n < 1$.

4.1. Leading-order expansion

The derivation of the asymptotic expansion follows the same sequence as for the classical approach (see Appendix A). At leading order, integration of the momentum equation (2.13) with the boundary condition (2.20) gives

$$\tau_{xz}^{(0)} = \frac{\lambda}{Bi}(h - z). \quad (4.1)$$

In the sheared layer, characterized by $|\boldsymbol{\tau}|^{(0)} > 1$ and $|\dot{\boldsymbol{\gamma}}|^{(0)} > 0$, the leading-order solution is assumed to correspond to a simple-shear flow (see below). Therefore, following the third condition in §2.1, the normal stresses vanish in this layer:

$$\tau_{xx}^{(0)} = \tau_{xx}^{Y(0)} = 0 \quad |\dot{\boldsymbol{\gamma}}|^{(0)} > 0 \quad (4.2)$$

with $|\dot{\boldsymbol{\gamma}}|^{(0)} = \partial_z u^{(0)}$ (where $\partial_z u^{(0)}$ is assumed to be always positive). The condition on the yield-stress tensor norm (2.17) then gives

$$\tau_{xy}^{Y(0)} = 1 \quad |\dot{\boldsymbol{\gamma}}|^{(0)} > 0. \tag{4.3}$$

From the constitutive relation (2.16), we thus obtain the following relation at leading order:

$$\frac{\lambda}{Bi}(h-z) = 1 + \frac{1}{Bi}\left(\partial_z u^{(0)}\right)^n \tag{4.4}$$

as long as $|\dot{\boldsymbol{\gamma}}|^{(0)} > 0$. Equation (4.4) implies that the leading-order strain rate $|\dot{\boldsymbol{\gamma}}|^{(0)}$ vanishes for $z = h - Bi/\lambda$. The fluid domain can thus be divided into two regions: a pseudo-plug layer with $|\dot{\boldsymbol{\gamma}}|^{(0)} = 0$ for $h - h_p \leqslant z \leqslant h$, and a fully sheared layer for $z \leqslant h - h_p$. The thickness h_p of the pseudo-plug layer is given by

$$h_p = \frac{Bi}{\lambda} \tag{4.5}$$

Taking into account the boundary condition (2.8), integration of (4.4) yields the leading-order velocity profile in the sheared layer:

$$u^{(0)} = \frac{n}{1+n}\lambda^{1/n}\left[\left(h-h_p\right)^{1+1/n} - \left(h-h_p-z\right)^{1+1/n}\right]. \tag{4.6}$$

The leading-order velocity in the pseudo-plug layer $u_{\mathrm{PP}}^{(0)}(x,t)$ should equal the value of the above expression at $z = h - h_p$, namely:

$$u_{\mathrm{PP}}^{(0)} = \frac{n}{1+n}\lambda^{1/n}\left(h-h_p\right)^{1+1/n}. \tag{4.7}$$

This leading-order velocity profile is thus identical to that obtained in the classical asymptotic expansion (section 3).

In the pseudo-plug, the constitutive equation at leading order reduces to $\tau_{xz}^{(0)} = \tau_{xz}^{Y(0)}$ and $\tau_{xx}^{(0)} = \tau_{xx}^{Y(0)}$. From expression (4.1) and the condition (2.17), we thus find

$$\tau_{xx}^{(0)} = \delta\sqrt{1 - \left(\frac{h-z}{h_p}\right)^2} \quad |\dot{\boldsymbol{\gamma}}|^{(0)} = 0, \tag{4.8}$$

with $\delta = \mathrm{sgn}(\tau_{xx})$. Accordingly, the normal stress is non-zero at leading order in the pseudo-plug and ensures that this layer is just on the verge of yielding: $|\boldsymbol{\tau}| = 1 + O(\varepsilon)$. Integration of the normal momentum balance (2.14) with the second dynamic boundary condition (2.21) and matching at the interface $z = h - h_p$ leads to the pressure profile:

$$p^{(0)} = \begin{cases} h - z & z < h - h_p \\ h - z - \delta Bi \dfrac{Fr^2}{Re}\sqrt{1 - \left(\dfrac{h-z}{h_p}\right)^2} & z \geqslant h - h_p \end{cases} \tag{4.9}$$

The leading-order pressure $p^{(0)}$ has a hydrostatic distribution in the Herschel-Bulkley sheared layer. In the pseudo-plug, however, the pressure includes an additional contribution due to the normal stress.

Lastly, the leading-order normal velocity $w^{(0)}$ can be derived from the integration of the continuity equation (2.12) with the no-penetration condition at the bottom (2.18) and matching at the interface $z = h - h_p$. This yields, for $0 \leqslant z \leqslant h - h_p$:

$$w^{(0)} = \lambda^{1/n}\left\{\frac{n}{1+n}\left[\left(h-h_p\right)^{1+1/n} - \left(h-h_p-z\right)^{1+1/n}\right] - z\left(h-h_p\right)^{1/n}\right\}\partial_x h \tag{4.10}$$

4.2. First-order correction

At $O(\varepsilon)$, the integration of the horizontal momentum equation (2.13) with the dynamic boundary condition (2.20) gives the following first-order correction for the shear stress $\tau_{xz}^{(1)}$

$$\tau_{xz}^{(1)} = 2\tau_{xx}^{(0)}\partial_x h - \frac{Re}{Bi}\int_z^h \left(\partial_t u^{(0)} + u^{(0)}\partial_x u^{(0)} + w^{(0)}\partial_z u^{(0)}\right) \mathrm{d}z + \frac{Re}{BiFr^2}(z-h)\partial_x h. \tag{4.11}$$

As explained previously and in [19], the stress is written as the sum of the yield-stress components and the viscous contribution, i.e. $\tau_{xz}^{(1)} = \tau_{xz}^{Y(1)} + \tau_{xz}^{v(1)}$. To define these parts, we follow the fourth condition discussed in §2.1, i.e, we put all the terms originating from the leading order normal stress to the yield-stress component $\tau_{xz}^{Y(1)}$ and all other terms to the viscous-stress components. The first-order correction to the viscous part then reads

$$\tau_{xz}^{v(1)} = -\frac{Re}{Bi}\int_z^h \left(\partial_t u^{(0)} + u^{(0)}\partial_x u^{(0)} + w^{(0)}\partial_z u^{(0)}\right) \mathrm{d}z + \frac{Re}{BiFr^2}(z-h)\partial_x h \tag{4.12}$$

while the first-order correction to the yield-stress tensor is $\tau_{xz}^{Y(1)} = 2\tau_{xx}^{Y(0)}\partial_x h$. The integral in (4.12) can be calculated analytically from the expressions of the leading-order solutions $u^{(0)}$ and $w^{(0)}$. In the pseudo-plug layer ($z \geqslant h - h_p$), we obtain

$$\tau_{xz\mathrm{PP}}^{v(1)} = \frac{Re}{Bi}(z-h)\left[\lambda^{1/n}\left(h-h_p\right)^{1/n}\partial_t h + \left(\frac{1}{Fr^2} + \frac{n}{1+n}\lambda^{2/n}\left(h-h_p\right)^{1+2/n}\right)\partial_x h\right] \tag{4.13}$$

while, for $z \leqslant h - h_p$, we obtain

$$\begin{aligned}\tau_{xz}^{v(1)} = {} & \frac{\lambda^{1/n}Re}{Bi}\left\{\frac{h-h_p-z}{1+n}\left[n\left(h-h_p-z\right)^{1/n} - (1+n)\left(h-h_p\right)^{1/n}\right] - h_p\left(h-h_p\right)^{1/n}\right\}\partial_t h \\ & + \frac{Re}{Bi}\left\{\frac{z-h}{Fr^2} + \frac{n}{(1+n)(1+2n)}\lambda^{2/n}\left(h-h_p\right)^{1/n}\right. \\ & \left.\times\left[\left(h-h_p-z\right)^{1+1/n}\left(2n\left(h-h_p\right)+z\right) - (1+2n)(h-z)\left(h-h_p\right)^{1+1/n}\right]\right\}\partial_x h\end{aligned} \tag{4.14}$$

Besides, at $O(\varepsilon)$, the constitutive equation (2.16) yields, for $z \leqslant h - h_p$:

$$\tau_{xz}^{v(1)} = \frac{n}{Bi}\left(\partial_z u^{(0)}\right)^{n-1}\partial_z u^{(1)}. \tag{4.15}$$

From equations (4.14) and (4.15), the first-order correction $u^{(1)}$ for $z < h - h_p$ can be integrated analytically:

$$\begin{aligned}u^{(1)} = {} & \frac{Re\lambda^{-1+2/n}}{(n+1)(n+2)}\left\{-n\left(h-h_p-z\right)^{1+2/n}\right. \\ & \left.+(n+2)\left(h-h_p\right)^{1/n}\left(h-h_p-z\right)^{1/n}\left(nh_p+h-z\right) - \left(h-h_p\right)^{2/n}\left[n(n+3)h_p+2h\right]\right\}\partial_t h \\ & + \frac{nRe\lambda^{-1+3/n}}{2(n+1)^2(n+2)(2n+1)}\left\{\left(h-h_p\right)^{1/n}\left(h-h_p-z\right)^{1/n}\left[2(n+2)(2n+1)\left(h-h_p\right)^{1+1/n}\left(h-z+nh_p\right)\right.\right. \\ & \left.\left.-\left(h-z-h_p\right)^{1+1/n}\left(n(5+4n)\left(h-h_p\right)+(2+n)z\right)\right] - \left(h-h_p\right)^{1+3/n}\left[(4+5n)h+n\left(9+14n+4n^2\right)h_p\right]\right\}\partial_x h \\ & + \frac{Re\lambda^{-1+1/n}}{(n+1)Fr^2}\left[\left(h-h_p-z\right)^{1/n}\left(h+nh_p-z\right) - \left(h-h_p\right)^{1/n}\left(h+nh_p\right)\right]\partial_x h.\end{aligned} \tag{4.16}$$

From equation (4.15), it is clear that the derivative $\partial_z u^{(1)}$ is equal to zero at the fake yield-surface $z = h - h_p$ when $n < 1$. In fact, as shown in Appendix D, the magnitude of $\partial_z u$ in the pseudo-plug is $O(\varepsilon^{2-n})$, and thus less than $O(\varepsilon)$

if $n < 1$. Accordingly, for $n < 1$, the first-order velocity correction in the pseudo-plug layer $u^{(1)}_{\mathrm{PP}}(t, x)$ does not depend on z and is expressed as:

$$u^{(1)}_{\mathrm{PP}} = -Re\lambda^{-1+2/n}\frac{\left(h-h_p\right)^{2/n}\left[n\left(n+3\right)h_p+2h\right]}{\left(n+2\right)\left(1+n\right)}\partial_t h - \frac{Re\lambda^{-1+1/n}}{\left(n+1\right)Fr^2}\left(h-h_p\right)^{1/n}\left(nh_p+h\right)\partial_x h \\ - \frac{Re\left(h-h_p\right)^{3/n+1}\lambda^{-1+3/n}}{2\left(n+1\right)^2\left(n+2\right)\left(2n+1\right)}\left[n^2\left(2n\left(2n+7\right)+9\right)h_p + nh\left(5n+4\right)\right]\partial_x h. \quad (4.17)$$

Let us note that the solution (4.16)-(4.17), with a constant velocity in the pseudo-plug at $O(\varepsilon)$, was already proposed in [16] to derive a shallow-flow model, although it was not consistent with the constitutive law considered in that paper. In contrast, in the framework of the alternative Herschel-Bulkley law proposed here, this solution is consistent up to the first order in ε.

Nevertheless, capturing a slight shear rate in the pseudo-plug seems desirable from a physical point of view. Recall that, for the case of Bingham fluids ($n = 1$), the expansions at first order include such a shearing effect [19]. Formally, equation (4.15) was obtained under the assumption $\partial_z u^{(0)} = O(1)$. This assumption is not satisfied close to the fake yield-surface, where $\partial_z u^{(0)}$ becomes very small. Consequently, other terms should be kept in the expansion of the strain rate $|\dot{\boldsymbol{\gamma}}|$, such that $|\dot{\boldsymbol{\gamma}}|$ does not vanish at $O(\varepsilon)$ in the pseudo-plug. The corresponding expansions are presented in Appendix D, but lead to a non-linear equation that cannot be integrated analytically. Since, again, our goal is to build analytical expansions, we propose below an alternative approach based on a 'Bingham plateau' regularization for the first-order expansion.

'Bingham plateau' regularization at $O(\varepsilon)$. To avoid the divergence of $|\partial_z u^{(0)}|^{n-1}$ at the fake yield surface in equation (4.15) and obtain non-zero shear rate at $O(\varepsilon)$ in the pseudo-plug layer while still obtaining integrable equations, we propose to regularize equation (4.15) as follows:

$$\tau^{v\,(1)}_{xz} = \frac{n}{Bi}\frac{\partial_z u^{(1)}}{\left(\partial_z u^{(0)}\right)^{1-n} + (\lambda\delta)^{1/n-1}}. \quad (4.18)$$

Here δ is a small regularization parameter of $O(\varepsilon^\beta)$, with $\beta > 0$, that plays the role of the thickness of a thin layer located between $z = h - h_p$ and $z = h - h_p - \delta$. In this layer, $\partial_z u^{(0)}$ and the constitutive equation at first order reduces to an effective Bingham rheology $\tau^{v\,(1)}_{xz} = \partial_z u^{(1)}/Bi^*$, with $Bi^* = (\lambda\delta)^{1/n-1}Bi/n$. Note that the small correction provided by δ in equation (4.18) does not contribute to the expansions up to $O(\varepsilon)$, since it results in a term of $O(\delta\varepsilon) = O(\varepsilon^{1+\beta})$. The first-order velocity term (4.17) thus remains unchanged. In the pseudo-plug ($z > h - h_p$), we extrapolate equation (4.18), thus having a 'Bingham plateau' at first order:

$$\tau^{v\,(1)}_{xz\mathrm{PP}} = \frac{1}{Bi^*}\partial_z u^{(1)}. \quad (4.19)$$

Equations (4.18) and (4.19) can be integrated analytically up to $O(\varepsilon^{1+\beta})$ taking into account the boundary conditions at the bottom. The full expression for $u^{(1)}$ is given in Appendix C.

Note that the 'Bingham plateau' approach is introduced only at $O(\varepsilon)$ to regularize the terms coming from the power-law viscous stress tensor, while the leading order velocity profile is not affected by the regularization. As shown in Appendix D, for specific values of δ the solution of Equations (4.18) and (4.19) provides effectively a good approximation of the solution obtained by integrating numerically the full non-linear equation resulting from the proper treatment of the alternative constitutive law in the vicinity of the fake yield surface.

5. Comparison with experiments

In this section, the longitudinal velocity profiles obtained with the two different asymptotic expansions derived above are cross-compared with experimental data. In the case of the classical formulation of the yield-stress tensor, we consider expansion (3.14), including all terms arising from the transition layer. For the alternative expression of Herschel-Bulkley law, we use the leading-order solution given by (4.6) and (4.7), and the first order correction given in Appendix C. Let us remind that the smooth expansion of the velocity profile for the classical rheology needs to be

Table 1
Parameters of the experiments, as reported in Chambon et al. [26]: yield stress τ_c (Pa), consistency K (Pa s^n), power-law index n, slope angle θ (deg.), steady uniform height H_N (mm), Bingham number Bi, Reynolds number Re, Froude number Fr, driving parameter λ, scaled theoretical pseudo-plug thickness h_p.

Exp.	τ_c	K	n	θ	H_N	Bi	Re	Fr	λ	h_p
HB1	13.3	9.8	0.40	15.3	14.6	1.13	0.044	0.061	3.219	0.35
HB3	13.3	9.8	0.40	15.3	16.2	0.95	0.098	0.095	3.003	0.32
HB13	8.0	6.0	0.43	15.3	15.5	0.5	1.37	0.39	2.455	0.20

computed numerically, whereas it is fully analytical for the alternative Herschel-Bulkley constitutive law. For the sake of comparison, we also consider the non-smooth expansion based on the classical rheology with simple matching, given by expressions (3.1) and (3.2).

The experimental dataset is described in [31] and [26]. Steady-state viscoplastic surges down an inclined slope were generated with a conveyor belt setup. High-resolution measurements of the internal velocity field within the surges and of the free-surface shape could be obtained. The depth-averaged velocity of the surges U is imposed and constant everywhere. Since the flows are steady, we can consider that the surge tip is located at $x = 0$, with the fluid occupying the negative part of the x-axis. In what follows, values of x thus correspond to the distance from the tip. The theoretical velocity profiles predicted by the asymptotic expansions are computed based on the values of h and $\partial_x h$ measured in the experiments. In the comparisons presented thereafter, the longitudinal velocity is normalized by the imposed depth-averaged velocity U, while values of x and z are normalized by the uniform flow depth observed far from the tip.

Figures 2-4 present comparisons between the predicted and measured velocity profiles for three sets of parameters indicated in Table 1. Note that, due to the difficulty of the measurements, experimental datapoints are sometimes lacking close to the free surface. To study the influence of the regularization parameter, predictions of the new expansion with different values of δ are shown, including the case $\delta = 0$. In the latter the shear rate is null everywhere in the pseudo-plug as clear from expression (4.17). It can be seen that all asymptotic expansions fit perfectly the experimental data in the uniform flow region far from the tip ($x = -10.16$ for HB1 and HB13, and $x = -10.07$ for HB3). In this region the typical two-layer flow structure is recovered, with an unsheared plug layer upon a sheared zone.

For $-5 < x < -1.9$, typically, the experimental data are consistent with the presence of a pseudo-plug zone characterized by slight shearing close to the free-surface. The asymptotic expansion with simple matching fails to capture this effect because of the unphysical kink and large shear rates close to the fake yield surface. The solution with asymptotic matching seems to slightly overestimate the shearing in the pseudo-plug, although the predictions are generally within the experimental error bars. The new expansion is in very good agreement with the data within this region for the different non-zero values of δ shown, though the case $\delta = 0$ is still in the error bar.

For $x > -1.2$, typically, i.e. close to the tip, the flow appears to be completely sheared within the whole fluid thickness, without clear pseudo-plug. In this region, both the predictions obtained with asymptotic matching and with the new expansion (for the non-zero values of δ) appear to reproduce the experimental data reasonably well. This is particularly clear in the case of Figure 4, for which experimental measurements could be obtained very close to the free surface. In Figures 2-3, experimental datapoints are lacking close to the free surface, but the predicted profiles are still within the error bars and capture the measured shearing in the zones where data are available. Prediction of the new expansion with $\delta = 0$ results in a null shearing in the pseudo-plug and is unable to properly capture the measured profiles close to the free surface. Conversely, excessively large values of δ lead to overestimation of the shearing. In general, "optimal" values of the parameter δ thus need to be determined on a case-by-case basis. In particular, it can be noted that this optimal value of δ seems to decrease when the Bingham number increases (compare Fig. 4 and 2). This presumably comes from the fact that the overall shearing within the surges decreases as the Bingham number increases.

Overall, the predictions provided by the two smooth velocity expansions are relatively close to one another, and both are in good agreement with the experimental data even close to the tip of the surges. It should be mentioned that both expansions have the same expressions at the leading order in the whole fluid domain, and at the first order in the sheared (Herschel-Bulkley) layer. Hence, obtaining relatively similar predictions is not necessarily surprising. Yet, the two approaches differ regarding the origin of shearing in the pseudo-plug. With the classical rheology, shearing

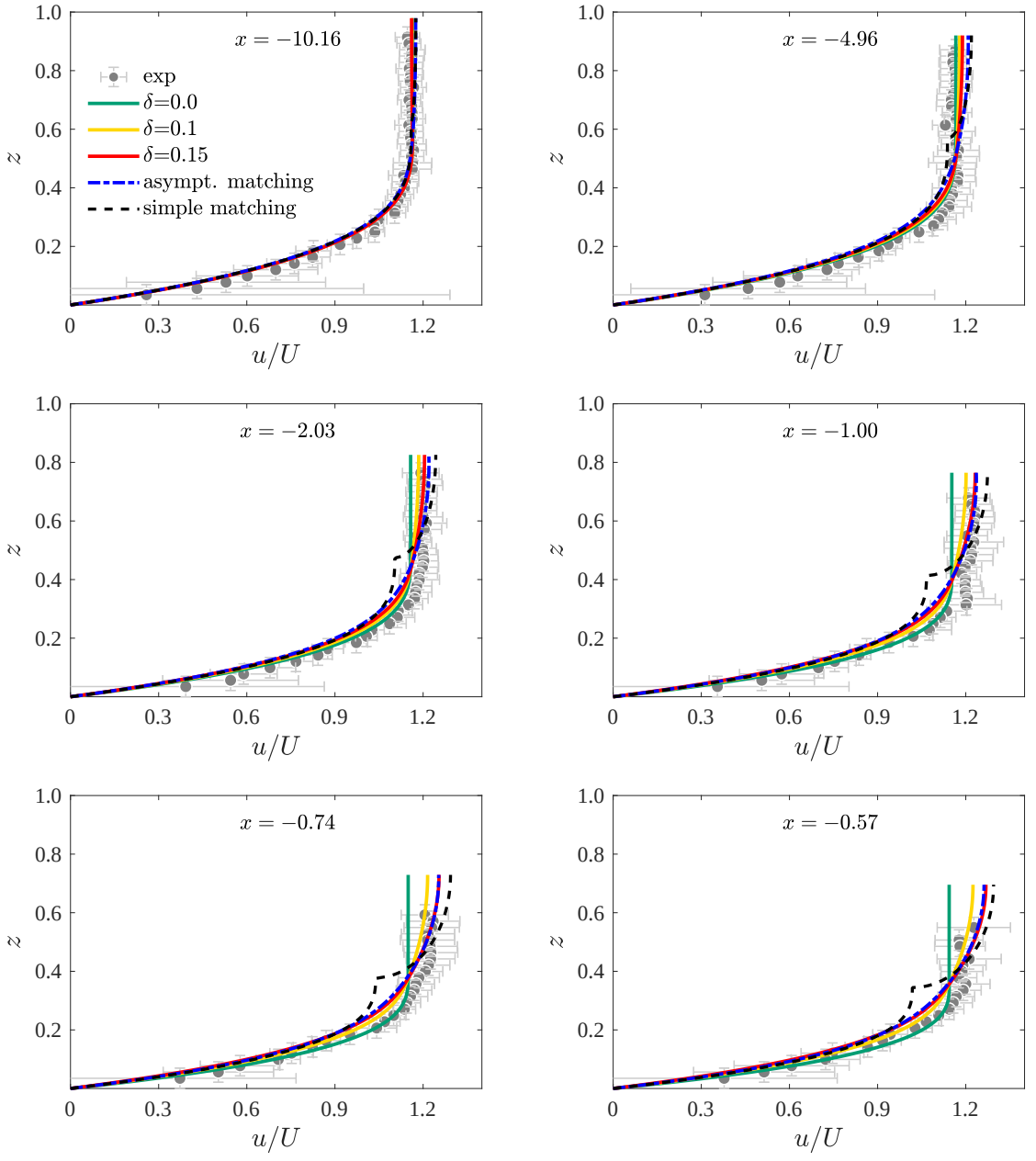

Figure 2: Experimental-theoretical comparisons for experiment HB1 (see Table 1): non-dimensional profiles of longitudinal velocity u normalized by the depth-averaged velocity U for six values of the distance from the tip x. Gray dots correspond to experimental measurements with associated error bars), the dashed and blue dot-dashed lines correspond to the classical expansion with simple and asymptotic matching, respectively, and the solid lines correspond to the new expansion with different values of δ (see legend).

in the pseudo-plug is driven by plastic effects, whereas with the alternative formulation it is driven by viscous effects. It can be argued, however, that the introduction of the asymptotic transition layer in the first approach mitigates this difference, since both plastic and viscous effects contribute to the shearing in this layer.

It can also be observed that the asymptotic expansion based on the classical rheology with asymptotic matching sometimes demonstrates a small negative shearing close to the free surface. This is visible, e.g., in Figure 4 at $x = -0.36$. This negative shearing occurs for small values of h_p: in this case the transition layer, with a thickness

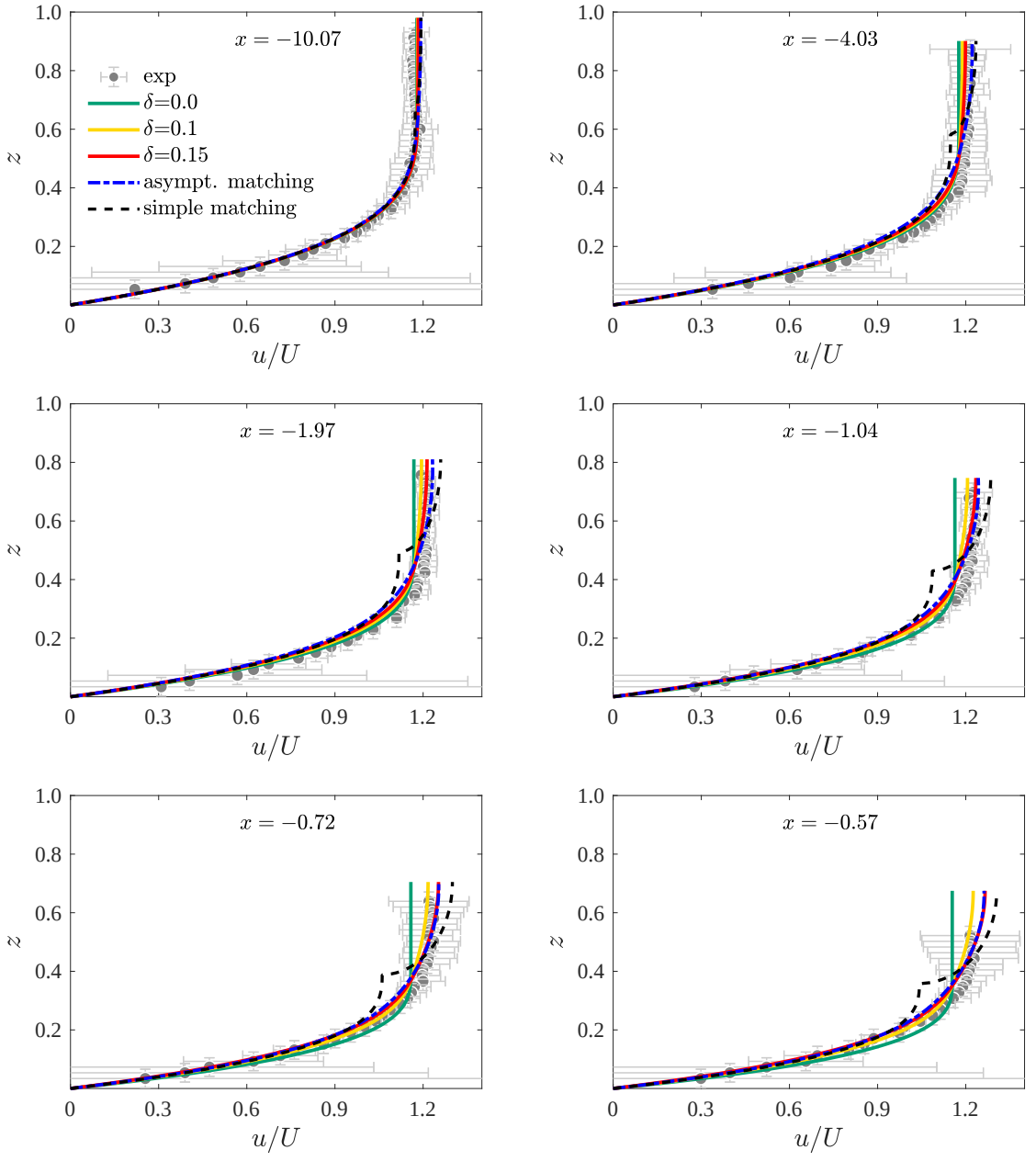

Figure 3: Experimental-theoretical comparison for experiment HB3 (see Table 1): same legend as Fig. 2.

formally of order $O(\varepsilon^{2n/(2+n)})$, can be thicker than the pseudo-plug and therefore extend up to the free surface. As a result, the combination with the first and smaller order terms of the pseudo-plug solution may result in unexpected behaviors.

In Appendix D, we also numerically compute the velocity profiles obtained in the framework of the alternative Herschel-Bulkley law without the Bingham plateau regularization, by using a specific matching procedure at the fake yield surface. In this case, the viscous stress tensor is treated properly close to the fake-yield surface but the solution is given by non-integrable equation. It is shown that this solution is in good agreement with the experiment. It is also found that, if a proper value of δ is chosen, the analytical expansion (C.1)-(C.7) provides an excellent approximation of the numerical solution obtained by this specific matching.

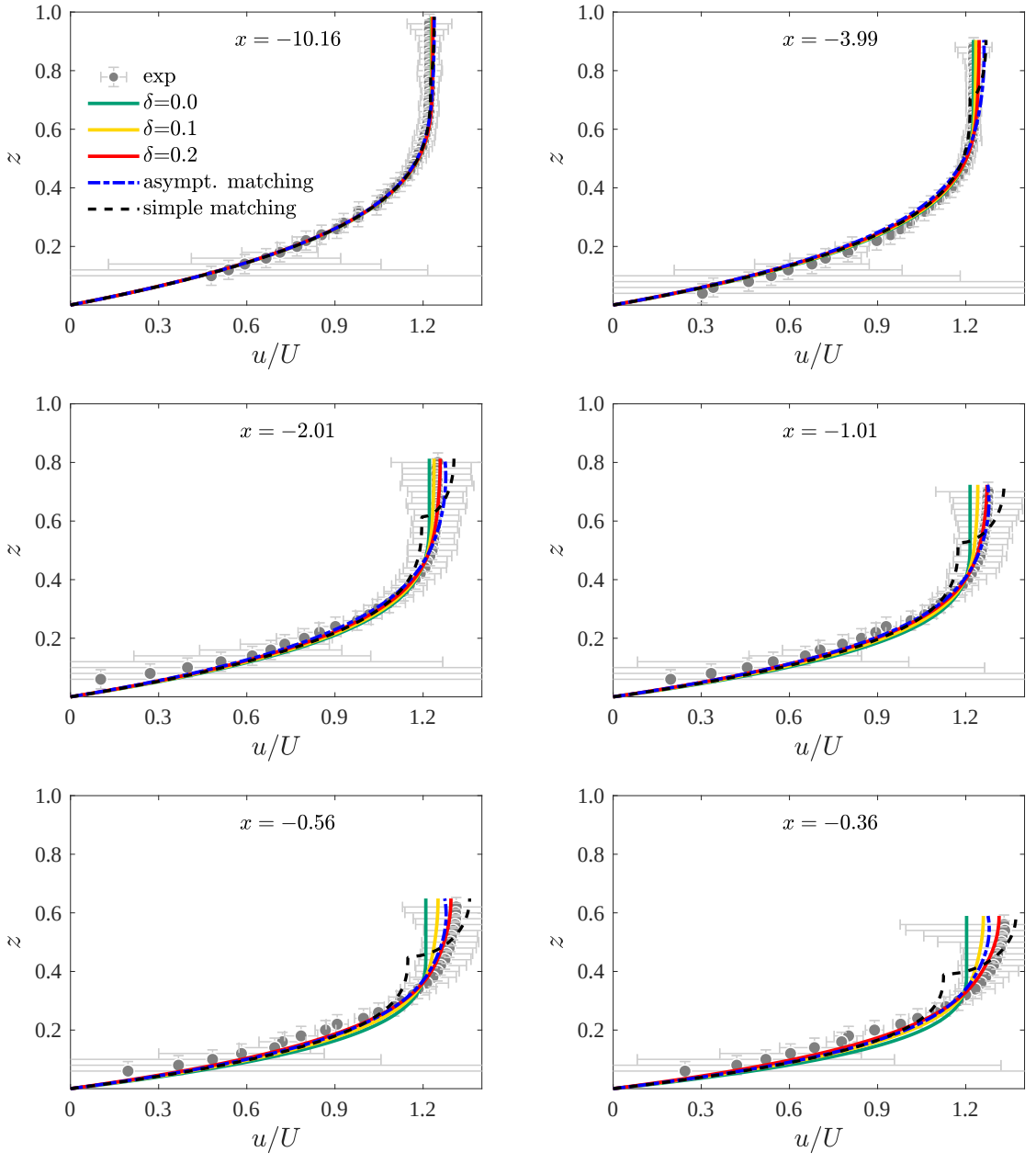

Figure 4: Experimental-theoretical comparison for experiment HB13 (see Table 1): same legend as Fig. 2.

6. Conclusions

In this study, smooth velocity expansions for Herschel–Bulkley flows down an inclined plane are constructed up to first order in the shallow-flow parameter ε. For the classical formulation of the constitutive law, an asymptotic matching procedure is used to avoid the divergence of the strain rate at the fake yield surface. The full solution in the transition layer is constructed for the first time. In particular, we show that proper matching with the first-order inertial terms in the sheared layer requires the addition of extra terms, the number of which depends on the power-law index n. The resulting expansion includes terms given by the non-integrable equations. Alternatively, a new version of the tensorial Herschel-Bulkley rheology is proposed, based on a specific regularization of the yield-stress tensor.

Specifically, the assumption of alignment between the yield-stress and the strain-rate tensors is removed. Note that this new regularization preserves a perfectly rigid behavior below the yield-stress. For $n = 1$, these assumptions were sufficient to construct fully analytical, smooth expansions of the velocity field [19]. For $n < 1$, however, a specific regularization is also needed to handle the power-law viscous stress tensor at $O(\varepsilon)$ and get a non-zero shearing in the pseudo-plug, as expected. These assumptions allow us to derive a smooth velocity expansion given by fully analytical expressions at first order ε. The leading order recovers the velocity profiles obtained for a classical Herschel-Bulkley fluid, while the regularization of the viscous term appears only at first order. Note that this regularization of the viscous stress tensor at $O(\varepsilon)$ can formally be avoided, but this would also lead to non-integrable equations for $n < 1$.

The constructed velocity expansions are compared with experimental data coming from free-surface surges generated in the laboratory. The theoretical velocity profiles are computed using the measured free-surface height. Overall, both expansions provide good agreement with the data, even close to the surge tip, where the shear rate becomes significant across the whole fluid layer. It is interesting to observe that expansions up to order $O(\varepsilon)$ are sufficient to capture this behaviour, although the shallow-flow assumption $\varepsilon \ll 1$becomes questionable close to the tip due to large free-surface gradients. Note also that taking h_p as constant in the expansions does not impede the capacity of these expansions at $O(\varepsilon)$ to predict velocity profiles, in which the effective pseudo-plug is confined close to the free surface or has disappeared. As expected, however, the leading-order expansion, and the first-order expansion based on the new rheological formulation with $\delta = 0$, show significant discrepancies with data close to the tip due to a null shear rate in the pseudo-plug layer. We also observed that the expansion based on the classical constitutive law with asymptotic matching tend to overestimate shearing in the pseudo-plug in some cases, and leads to unrealistic predictions in configurations where the effective thickness of the transition layer becomes non-negligible compared to that of the pseudo-plug. On the other hand, the predictions of the expansion based on the alternative formulation of the rheology are sensitive to the choice of the regularization parameter δ, which controls the size of the Bingham layer at first order. Furthermore, the optimal value of this parameter appears to depend on the Bingham number.

Since the two expansions are identical at leading-order in the whole fluid domain, and at first-order in the sheared layer, we can expect them to provide similar predictions in a wide range of flow configurations. The main advantage of the expansion based on the new formulation of the rheology, including regularization of the viscous stress tensor at $O(\varepsilon)$ when $n < 1$, is that it is fully analytical. Hence, this expansion can directly be used to derive closed-form shallow-flow models with a well-posed mathematical structure, generalizing the work already performed for Bingham fluids [19]. The derivation of such a model for general values of n is currently under progress. Finally, let us recall that, even if this approach involves mathematical regularizations of the constitutive law, the existence of the yield threshold and the rigid behaviour below this threshold, are preserved. This feature is essential to derive models that can predict the stoppage of the flows. To conclude, it is worth reiterating the numerous technical difficulties that arise when attempting to derive asymptotic expansions using the classical tensorial extension of the Herschel-Bulkley law. These difficulties arise from the divergence of both the yield-stress and the viscous terms as the shear rate goes to zero. Our work shows that these difficulties can be mitigated by alternative assumptions on the constitutive law, which lead to results that are essentially identical or even more relevant than with the classical approach. This may pave the way for the formulation of new viscoplastic laws with better mathematical properties, while at the same time better representing the rheology of real yield-stress fluids (e.g., normal stress differences).

Acknowledgements

This work has received funding from the European Union's Horizon 2020 research and innovation programme under the Marie Skłodowska-Curie grant agreement No 955605.

A. Classical expansions with simple matching

Here we derive the shallow-flow expansions for Herschel-Bulkley fluids described by the constitutive law (2.1) with the classical representation of the yield-stress tensor (2.3). The variables are expanded according to (2.23), and we consider the resulting equations at each order.

Leading order

At $O(1)$ with respect to ϵ, integration of the momentum balance (2.13) gives

$$\tau_{xy}^{(0)} = \frac{\lambda}{Bi}(h-z). \tag{A.1}$$

The leading order strain rate is $|\dot{\boldsymbol{\gamma}}|^{(0)} = \partial_z u^{(0)}$. Thus, if $\partial_z u^{(0)} \neq 0$, the constitutive equation (2.16) with (2.3) gives

$$\frac{\lambda}{Bi}(h-z) = 1 + \frac{1}{Bi}\left(\partial_z u^{(0)}\right)^n. \tag{A.2}$$

As clear from (A.2), the leading order strain rate $|\dot{\boldsymbol{\gamma}}|^{(0)} = \partial_z u^{(0)}$ is a decreasing function of z, maximum at the bottom and vanishing at $z = h - Bi/\lambda$. We thus expect the existence of a pseudo-plug of thickness $h_p = Bi/\lambda$, in which the strain rate is of $O(\epsilon)$ and the leading-order longitudinal velocity $u^{(0)}(x,t)$ does not depend on z. Then, integration of (A.2) with the bottom boundary condition gives the profile

$$u^{(0)} = \frac{n}{n+1}\lambda^{\frac{1}{n}} \begin{cases} (h-h_p)^{\frac{n+1}{n}} - (h-h_p-z)^{\frac{n+1}{n}} & z < h-h_p, \\ (h-h_p)^{\frac{n+1}{n}} & z \geqslant h-h_p, \end{cases} \tag{A.3}$$

where the expression in the pseudo-plug is obtained by assuming velocity continuity at the fake yield surface $z = h - h_p$.

The leading-order normal stress $\tau_{xx}^{(0)}$ in the sheared layer is obviously zero, from the constitutive equations (2.15)–(2.3). On the contrary, in the pseudo-plug the leading-order solution is expected to be at the yielding threshold, namely $|\boldsymbol{\tau}|^{(0)} = 1$. From this and (A.1), a non-zero normal stress is obtained in the pseudo-plug, such that

$$\tau_{xx}^{(0)} = \begin{cases} 0 & z < h-h_p, \\ \delta\sqrt{1-\left(\dfrac{h-z}{h_p}\right)^2} & z \geqslant h-h_p. \end{cases} \tag{A.4}$$

Here δ corresponds to sign of the normal stress, which will be defined below.

The leading-order pressure $p^{(0)}$ is found from integration of the momentum equation (2.14), completed by the dynamic boundary condition (2.21), which leads to

$$p^{(0)} = \begin{cases} h-z & z < h-h_p, \\ h-z-\delta Bi\dfrac{Fr^2}{Re}\sqrt{1-\left(\dfrac{h-z}{h_p}\right)^2} & z \geqslant h-h_p. \end{cases} \tag{A.5}$$

Note that the leading-order pressure in the pseudo-plug is not hydrostatic because of the normal stress contribution.

Finally, integration of the mass equation (2.12), completed by the no-penetration condition at the bottom and the continuity condition at the fake yield surface, gives the profile for the normal velocity:

$$w^{(0)} = \lambda^{\frac{1}{n}} \begin{cases} \dfrac{n}{n+1}\left((h-h_p)^{\frac{n+1}{n}} - (h-h_p-z)^{\frac{n+1}{n}}\right)\dfrac{\partial h}{\partial x} - z(h-h_p)^{\frac{1}{n}}\dfrac{\partial h}{\partial x} & z < h-h_p, \\ \dfrac{n}{n+1}(h-h_p)^{\frac{n+1}{n}}\dfrac{\partial h}{\partial x} - z(h-h_p)^{\frac{1}{n}}\dfrac{\partial h}{\partial x} & z \geqslant h-h_p. \end{cases}$$

First-order corrections

At $O(\epsilon)$, integration of the momentum balance (2.13) gives

$$\tau_{xy}^{(1)} = 2\tau_{xx}^{(0)} + \frac{1}{Bi}\left(\mathcal{I}(z) + \mathcal{P}(z)\right), \tag{A.6}$$

where the inertial $\mathcal{I}$ and hydrostatic pressure $\mathcal{P}$ corrections are given by

$$\mathcal{I}(z) = -Re \int_z^h \left(\partial_t u^{(0)} + u^{(0)} \partial_x u^{(0)} + w^{(0)} \partial_z u^{(0)} \right) dz, \quad \mathcal{P}(z) = \frac{Re}{Fr^2}(z-h)\partial_x h. \tag{A.7}$$

The integral term $\mathcal{I}$ can be calculated analytically. Note that the integrand of this term presents a discontinuity at the fake-yield surface, which should be carefully taken into account.

Let us first consider the sheared layer. The constitutive law (2.16) at first order gives

$$n \left(\partial_z u^{(0)} \right)^{n-1} \partial_z u^{(1)} = \tau_{xz}^{(1)}, \tag{A.8}$$

which together with the bottom boundary condition provides, for $z < h - h_p$,

$$u^{(1)} = \frac{1}{n} \int_0^z \lambda^{\frac{1-n}{n}} \left(h - h_p - z \right)^{\frac{1-n}{n}} \left[\mathcal{I}(z) + P(z) \right] dz. \tag{A.9}$$

In the pseudo-plug, the constitutive law (2.16) at leading order gives

$$\frac{\lambda}{Bi}(h-z) = \frac{\partial_z u^{(1)}}{\sqrt{\left(\partial_z u^{(1)} \right)^2 + 4 \left(\partial_x u^{(0)} \right)^2}}, \tag{A.10}$$

which together with the continuity condition at the fake yield surface provides, for $z \geqslant h - h_p$,

$$u^{(1)} = 2h_p \sqrt{1 - \left(\frac{h-y}{h_p} \right)^2} \left| \partial_x u_{pl}^{(0)} \right| - u_{sh}^{(1)}{}_{|z=h-h_p}. \tag{A.11}$$

Here the term $u_{sh}^{(1)}$ corresponds to the solution in the sheared layer.

Finally, to define δ, we can consider the constitutive equation (2.15) at leading order in the pseudo-plug:

$$\delta \sqrt{1 - \left(\frac{h-z}{h_p} \right)^2} = \frac{2\partial_x u^{(0)}}{\sqrt{\left(\partial_z u^{(1)} \right)^2 + 4 \left(\partial_x u^{(0)} \right)^2}}. \tag{A.12}$$

From this, given the expressions (A.3) and (A.11), we find: $\delta = \mathrm{sgn}(\partial_x h)$.

B. Classical expansions with asymptotic matching

Transition layer expansions

To overcome the impossibility to properly match the one-term expansion (3.7) in the transition layer with the sheared layer at $O(\varepsilon)$ (see 3.2), let us instead assume a two-term expansion for the velocity in the transition layer:

$$u = u_{pl}^{(0)}(x,t) + \varepsilon^{\alpha_1+\kappa} U_1(x,\xi,t) + \varepsilon^{\alpha_2+\kappa} U_2(x,\xi,t) + \dots \tag{B.1}$$

where $0 < \alpha_1 < 1$ and $\alpha_2 > \alpha_1$. The zoomed-in variable ξ is defined as in (3.8). Accordingly the expansion for the velocity derivative reads

$$\partial_z u = \varepsilon^{\alpha_1} S_1(x,\xi,t) + \varepsilon^{\alpha_2} S_2(x,\xi,t) + \dots \tag{B.2}$$

with S_1 and S_2 the derivatives of U_1 and U_2 with respect to ξ, respectively. The shear stress (2.16) can then be expressed as follows

$$\tau_{xz} = 1 - 2\varepsilon^{2(1-\alpha_1)}\frac{\left(\partial_x u_{pl}^{(0)}\right)^2}{{S_1}^2} + 4\varepsilon^{2-3\alpha_1+\alpha_2}\frac{\left(\partial_x u_{pl}^{(0)}\right)^2 S_2}{{S_1}^3} + \dots$$
$$+ \frac{1}{Bi}\left[\varepsilon^{n\alpha_1}{S_1}^n + n\varepsilon^{(n-1)\alpha_1+\alpha_2}\frac{S_2}{{S_1}^{1-n}} + 2(n-1)\varepsilon^{2+(n-2)\alpha_1}\frac{\left(\partial_x u_{pl}^{(0)}\right)^2}{{S_1}^{2-n}} + \dots\right] \quad \text{(B.3)}$$

At lowest order momentum balance gives equation (3.11) for $S_1(\xi)$. Accordingly α_1 and κ are defined by

$$\alpha_1 = \frac{2}{2+n}, \qquad \kappa = \frac{2n}{2+n}, \quad \text{(B.4)}$$

with the following equation for S_1

$$S_1^n + \lambda\xi = 2\frac{Bi}{S_1^2}\left(\partial_x u_{pl}^{(0)}\right)^2. \quad \text{(B.5)}$$

Let us assume for now that $n > 2/3$. In this case, the last term in (B.3) is $o(\varepsilon)$ and can be disregarded. At the next order, momentum balance thus yields

$$\frac{\varepsilon}{Bi}\Big[\mathcal{I}(h_s) + P(h_s)\Big] = 4\varepsilon^{2-3\alpha_1+\alpha_2}\left(\partial_x u_{pl}^{(0)}\right)^2\frac{S_2}{{S_1}^3} + \frac{n\varepsilon^{(n-1)\alpha_1+\alpha_2}}{Bi}\frac{S_2}{{S_1}^{1-n}}. \quad \text{(B.6)}$$

where we denote $h_s = h - h_p$. Balancing the terms implies

$$\alpha_2 = \frac{4-n}{2+n}, \quad \text{(B.7)}$$

and the following equation is obtained for the function S_2:

$$S_2 = \Big[\mathcal{I}(h_s) + P(h_s)\Big]\frac{{S_1}^3}{n{S_1}^{n+2} + 4Bi\left(\partial_x u_{pl}^{(0)}\right)^2}. \quad \text{(B.8)}$$

If however $n \leq 2/3$, the last term in (B.3) cannot be disregarded, and cannot be balanced with a corresponding term in the momentum balance. Furthermore, as will be shown below, an additional term of same weight also appears in the plastic part of the stress from higher-order products. To deal with these additional terms, we propose to add yet another term in the transition layer velocity expansion:

$$u = u_{pl}^{(0)}(x,t) + \varepsilon^{\alpha_1+\kappa}U_1(x,\xi,t) + \varepsilon^{\alpha_p+\kappa}U_p(x,\xi,t) + \varepsilon^{\alpha_2+\kappa}U_2(x,\xi,t) + \dots \quad \text{(B.9)}$$

where a priori $\alpha_1 < \alpha_p < \alpha_2$. Thus

$$\partial_z u = \varepsilon^{\alpha_1}S_1(x,\xi,t) + \varepsilon^{\alpha_p}S_p(x,\xi,t) + \varepsilon^{\alpha_2}S_2(x,\xi,t)\dots \quad \text{(B.10)}$$

with S_p the derivative of U_p with respect to ξ, and the expression for the shear stress now reads:

$$\tau_{xz} = 1 - 2\varepsilon^{2(1-\alpha_1)}\frac{\left(\partial_x u_{pl}^{(0)}\right)^2}{{S_1}^2}$$
$$+ 6\varepsilon^{4(1-\alpha_1)}\frac{\left(\partial_x u_{pl}^{(0)}\right)^4}{{S_1}^4} + 4\varepsilon^{2(1-\alpha_1)+(\alpha_2-\alpha_1)}\frac{\left(\partial_x u_{pl}^{(0)}\right)^2 S_2}{{S_1}^3} + 4\varepsilon^{2(1-\alpha_1)+(\alpha_p-\alpha_1)}\frac{\left(\partial_x u_{pl}^{(0)}\right)^2 S_p}{{S_1}^3} + \dots$$
$$+ \frac{1}{Bi}\left[\varepsilon^{n\alpha_1}{S_1}^n + 2(n-1)\varepsilon^{2+(n-2)\alpha_1}\frac{\left(\partial_x u_{pl}^{(0)}\right)^2}{{S_1}^{2-n}} + n\varepsilon^{n\alpha_1+(\alpha_2-\alpha_1)}\frac{S_2}{{S_1}^{1-n}} + n\varepsilon^{n\alpha_1+(\alpha_p-\alpha_1)}\frac{S_p}{{S_1}^{1-n}} + \dots\right] \quad \text{(B.11)}$$

Note that in the above expression, we heuristically disregarded all cross-products between terms in ε^{α_p} and in ε^{α_1} or ε^{α_2} for the moment (see below). The previous relation for S_1, S_2, α_1 and α_2 remain valid if all terms $O(\varepsilon^{4(1-\alpha_1)})$ effectively compensate in (B.11). This compensation imposes

$$6\varepsilon^{4(1-\alpha_1)}\frac{\left(\partial_x u_{pl}^{(0)}\right)^4}{{S_1}^4}+4\varepsilon^{2(1-\alpha_1)+(\alpha_p-\alpha_1)}\frac{\left(\partial_x u_{pl}^{(0)}\right)^2 S_p}{{S_1}^3}+\frac{1}{Bi}\left[2(n-1)\varepsilon^{2+(n-2)\alpha_1}\frac{\left(\partial_x u_{pl}^{(0)}\right)^2}{{S_1}^{2-n}}+n\varepsilon^{n\alpha_1+(\alpha_p-\alpha_1)}\frac{S_p}{{S_1}^{1-n}}\right]=0 \tag{B.12}$$

which leads to

$$\alpha_p=\frac{2(n+1)}{n+2}. \tag{B.13}$$

The following relation is then obtained for the function S_p:

$$S_p=\frac{\left(\partial_x u_{pl}^{(0)}\right)^2}{S_1}\,\frac{2(1-n){S_1}^{2+n}-6Bi\left(\partial_x u_{pl}^{(0)}\right)^2}{n{S_1}^{2+n}+4Bi\left(\partial_x u_{pl}^{(0)}\right)^2}. \tag{B.14}$$

Note that $\alpha_p<\alpha_2$ if $n<2/3$, as expected. It can also be shown that all higher-order cross-products and terms involving α_p in (B.11) are at least $O(\varepsilon^{6(1-\alpha_1)})$. These terms can thus effectively be disregarded for $n>2/5$. For $n\leq 2/5$, however, these cross terms would have to be accounted for, in addition to terms coming purely from the ε^{α_1} term in the velocity expansion. In this case, the above procedure could be repeated by adding a fourth term to the velocity expansion, and thence iteratively as n becomes smaller and smaller. We limit consideration here to the range $2/5<n\leq 2/3$, for which the above three-term expansion is sufficient. This range of n corresponds to that typically observed in the experiments (see section 5). Note that the case $n>2/3$ is retrieved by simply discarding all terms involving S_p.

Matching with the sheared and pseudo-plug layers

Let us explore the limits of the transition layer expansion for $\xi\to-\infty$ and $\xi\to\infty$, which should match with the expansions in the sheared and pseudo-plug layers, respectively. For $\xi\to-\infty$, we have $S_1\to(-\lambda\xi)^{1/n}$. Accordingly (B.8) gives

$$S_2\to\left[\mathcal{I}(h_s)+P(h_s)\right]\frac{(-\lambda\xi)^{\frac{1-n}{n}}}{n} \tag{B.15}$$

and (B.14) gives

$$S_p\to\frac{2(1-n)}{n}\left(\partial_x u_{pl}^{(0)}\right)^2(-\lambda\xi)^{-1/n}. \tag{B.16}$$

Using expression (3.8) to replace the zoomed variable ξ, the limit of the three-terms expansion of $\partial_z u$ in the transition layer, for $\xi\to-\infty$, thus reads

$$\partial_z u\to\lambda^{\frac{1}{n}}(h_s-z)^{\frac{1}{n}}+\varepsilon\frac{\lambda^{\frac{1-n}{n}}}{n}\left[\mathcal{I}(h_s)+P(h_s)\right](h_s-z)^{\frac{1-n}{n}}+\varepsilon^2\frac{2(1-n)}{n}\left(\partial_x u_{pl}^{(0)}\right)^2\lambda^{-1/n}(h_s-z)^{-1/n}+\ldots \tag{B.17}$$

The first term of (B.17) exactly matches the derivative of the leading-order solution (3.1) in the sheared layer. Similarly, it can be shown that the second term of (B.17) matches the first-order correction in the sheared-layer at $O(\varepsilon)$. The last term of (B.17), associated to S_p, only contributes at $O(\varepsilon^2)$ for $\xi\to-\infty$.

For $\xi\to+\infty$, i.e. in the pseudo-plug, we expect $S_1\to 0$. Accordingly, equation (B.5) for the function S_1 gives

$${S_1}^2\to 2\frac{h_p}{\xi}\left(\partial_x u_{pl}^{(0)}\right)^2 \tag{B.18}$$

Equation (B.8) for S_2 then leads to

$$S_2 \to \frac{1}{Bi\sqrt{2}}\left(\frac{h_p}{\xi}\right)^{3/2}\Big[\mathcal{I}(h_s)+P(h_s)\Big]\partial_x u_{pl}^{(0)}. \tag{B.19}$$

while (B.14) leads to

$$S_p \to= -\frac{3}{2}\left(\frac{\lambda\xi}{2Bi}\right)^{1/2}\left|\partial_x u_{pl}^{(0)}\right|. \tag{B.20}$$

Thus the limit of $\partial_z u$ for $\xi \to +\infty$ takes the form

$$\partial_z u \to \varepsilon\sqrt{\frac{2h_p}{z-h_s}}\left|\partial_x u_{pl}^{(0)}\right| + \frac{\varepsilon^2}{Bi\sqrt{2}}\left(\frac{h_p}{z-h_s}\right)^{3/2}\Big[\mathcal{I}(h_s)+P(h_s)\Big]\partial_x u_{pl}^{(0)} - \varepsilon\frac{3}{2}\sqrt{\frac{z-h_s}{2h_p}}\left|\partial_x u_{tl}^{(0)}\right| + \dots \tag{B.21}$$

Note that both the terms associated to S_1 and to S_p contribute at $O(\varepsilon)$ in this limit. In the pseudo-plug, the expression of the first-order derivative (3.4) diverges as $z \to h_s$. This precludes a direct matching with the transition layer. Let us thus introduce an intermediate variable $z_\eta = (z-h_s)/\varepsilon^\eta$, with $0 < \eta < \kappa$. In terms of this new variable, expression (B.21) becomes

$$\partial_z u \to \varepsilon^{1-\eta/2}\sqrt{\frac{2h_p}{z_\eta}}\left|\partial_x u_{pl}^{(0)}\right| + \frac{\varepsilon^{2-3\eta/2}}{Bi\sqrt{2}}\left(\frac{h_p}{z_\eta}\right)^{3/2}\Big[\mathcal{I}(h_s)+P(h_s)\Big]\partial_x u_{pl}^{(0)} - \varepsilon^{1+\eta/2}\frac{3}{2}\sqrt{\frac{z_\eta}{2h_p}}\left|\partial_x u_{pl}^{(0)}\right| + \dots \tag{B.22}$$

while expression (3.4) for $z > h_s$ reads

$$\partial_z u = \varepsilon^{1-\eta/2}\sqrt{\frac{2h_p}{z_\eta}}\left|\partial_x u_{pl}^{(0)}\right| + \frac{3\varepsilon^{1+\eta/2}}{2}\sqrt{\frac{z_\eta}{2h_p}}\left|\partial_x u_{pl}^{(0)}\right| + \dots . \tag{B.23}$$

Obviously, the first terms of the expansions are effectively matched. Interestingly, the second term in (B.23) also appears to match with the term associated to S_p in (B.22). The second term in (B.22), associated to S_2, does not appear to match with a corresponding term in (B.23). As this term is responsible for an $O(\varepsilon^2)$ contribution in (B.21), we can anticipate that a proper matching would require an expansion of $\partial_z u$ up to this order in the pseudo-plug.

Composite approximations

In the terminology of asymptotic matching [32], the expansions in the transition layer constitute inner solutions, while the expansions in the sheared layer and the pseudo-plug are outer solutions. Composite approximations of $\partial_z u$ can be obtained by adding the outer and inner solutions and subtracting their common matching terms. In the sheared layer, ie for $z < h_s$, this leads to:

$$\begin{aligned}\partial_z u = {} & \lambda^{\frac{1}{n}}(h_s-z)^{\frac{1}{n}} + \frac{\varepsilon}{n}\lambda^{\frac{1-n}{n}}(h_s-z)^{\frac{1-n}{n}}\Big[\mathcal{I}(z)+P(z)\Big] - \lambda^{\frac{1}{n}}(h_s-z)^{\frac{1}{n}} - \frac{\varepsilon}{n}\lambda^{\frac{1-n}{n}}(h_s-z)^{\frac{1-n}{n}}\Big[\mathcal{I}(h_s)+P(h_s)\Big] \\ & + \varepsilon^{\frac{2}{2+n}}S_1\left(\frac{z-h_s}{\varepsilon^{\frac{2n}{2+n}}}\right) + \varepsilon^{\frac{2(n+1)}{n+2}}S_p\left(\frac{z-h_s}{\varepsilon^{\frac{2n}{2+n}}}\right) + \varepsilon^{\frac{4-n}{2+n}}S_2\left(\frac{z-h_s}{\varepsilon^{\frac{2n}{2+n}}}\right).\end{aligned} \tag{B.24}$$

Note that we did not include the matching term associated to S_p, since this term is $O(\varepsilon^2)$ as shown above. In order to keep the contributions from the sheared layer explicit, the above expression can be rewritten under the form of an ordered expansion as follows:

$$\begin{aligned}\partial_z u = {} & \lambda^{\frac{1}{n}}(h_s-z)^{\frac{1}{n}} + \varepsilon^{\frac{2}{2+n}}S_1\Big[1-(1-R_1)^{\frac{1}{n}}\Big] + \frac{\varepsilon}{n}\lambda^{\frac{1-n}{n}}(h_s-z)^{\frac{1-n}{n}}\Big[\mathcal{I}(z)+P(z)\Big] \\ & + \varepsilon^{\frac{2(n+1)}{n+2}}\frac{\left(\partial_x u_{pl}^{(0)}\right)^2}{S_{t1}}\,\frac{2(1-n)-3R_1}{n+2R_1} + \varepsilon^{\frac{4-n}{2+n}}\frac{1}{n}\Big[\mathcal{I}(h_s)+P(h_s)\Big]\Big[\frac{n}{n+2R_1}-(1-R_1)^{\frac{1-n}{n}}\Big]S_1^{1-n}\end{aligned} \tag{B.25}$$

where we defined

$$R_1 = 2Bi\left(\partial_x u_{pl}^{(0)}\right)^2 S_1^{-(n+2)} \tag{B.26}$$

and made use of (B.5), (B.8) and (B.14) to express the differences between the transition layer terms and their respective limits in the sheared layer (matching terms) in (B.24). The above expression makes it clear that the transition layer is responsible for a contribution intermediate between $O(1)$ and $O(\varepsilon)$, as well as two additional contributions intermediate between $O(\varepsilon)$ and $O(\varepsilon^2)$ (in the range of n considered). The contributions are only "active" in the transition layer. Outside of the transition layer, we expect $S_1 = O(\varepsilon^{-2/(2+n)})$ and $R_1 = O(\varepsilon^2)$. Accordingly, the terms arising from the transition layer in (B.25) become $O(\varepsilon^2)$ and $O(\varepsilon^3)$ and can be disregarded at $O(\varepsilon)$, as expected.

In the pseudo-plug, for $z > h_s$, the composite approximation of $\partial_z u$ reads:

$$\begin{aligned}\partial_z u = \varepsilon\left[\frac{2(h-z)/h_p}{\sqrt{1-((h-z)/h_p)^2}} - \sqrt{\frac{2}{1-(h-z)/h_p}} + \frac{3}{2}\sqrt{\frac{1-(h-z)/h_p}{2}}\right]\left|\partial_x u_{pl}^{(0)}\right| \\ + \varepsilon^{\frac{2}{2+n}} S_1\left(\frac{z-h_s}{\varepsilon^{\frac{2n}{2+n}}}\right) + \varepsilon^{\frac{2(n+1)}{n+2}} S_p\left(\frac{z-h_s}{\varepsilon^{\frac{2n}{2+n}}}\right) + \varepsilon^{\frac{4-n}{2+n}} S_2\left(\frac{z-h_s}{\varepsilon^{\frac{2n}{2+n}}}\right)\end{aligned} \tag{B.27}$$

Here we did not include the matching term associated to S_2, since this term is $O(\varepsilon^2)$. Note also that the difference between the first two terms in (B.27) tends to zero as $z \to h_s$, showing that the introduction of the transition layer effectively suppresses the divergence of the strain rate at the fake yield surface. Similar as above, (B.27) can be rewritten under the form of an ordered expansion as follows:

$$\begin{aligned}\partial_z u = \varepsilon^{\frac{2}{2+n}} S_1\left[1-\sqrt{\frac{R_1}{R_1-1}}\right] + \varepsilon\frac{2(h-z)/h_p}{\sqrt{1-((h-z)/h_p)^2}}\left|\partial_x u^{(0)}\right| \\ + \varepsilon^{\frac{2(n+1)}{n+2}}\frac{\left(\partial_x u_{pl}^{(0)}\right)^2}{S_{t1}}\left[\frac{2(1-n)-3R_1}{n+2R_1} + \frac{3}{2}\sqrt{\frac{R_1-1}{R_1}}\right] + \varepsilon^{\frac{4-n}{2+n}}\left[\mathcal{I}(h_s)+P(h_s)\right]\frac{S_1^{1-n}}{n+2R_1}\end{aligned} \tag{B.28}$$

Here again, the transition layer is responsible for a contribution larger than $O(\varepsilon)$, and two additional contributions intermediate between $O(\varepsilon)$ and $O(\varepsilon^2)$ (in the range of n considered). Outside of the transition layer, we expect $S_1 = O(\varepsilon^{n/(n+2)})$ and $R_1 = O(\varepsilon^{-n})$, so that all terms associated to the transition layer become smaller than $O(\varepsilon)$. Note however that the contributions associated to S_1 and S_p are still larger than $O(\varepsilon^2)$, i.e. larger than in the sheared layer, while the contribution associated to S_2 is $O(\varepsilon^2)$.

Construction of the velocity profiles

The two expansions (B.25) and (B.28) can be integrated with the bottom boundary condition $u(0) = 0$ to obtain the longitudinal velocity field. This leads to (3.14), where the functions C, T, and D are defined as follows:

$$C(z) = \int_0^{(z-h_s)/\varepsilon^\kappa} S_1(a) \times \begin{cases} \left(1-(1-R_1(a))^{1/n}\right)da & z < h_s, \\ \left(1-\sqrt{\dfrac{R_1(a)}{R_1(a)-1}}\right)da & z \geqslant h_s, \end{cases} \tag{B.29}$$

$$T(z) = \int_0^{(z-h_s)/\varepsilon^\kappa} \frac{\left(\partial_x u_{pl}^{(0)}\right)^2}{S_1(a)} \times \begin{cases} \dfrac{2(1-n)-3R_1(a)}{n+2R_1(a)}da & z < h_s, \\ \left(\dfrac{2(1-n)-3R(a)}{n+2R_1(a)} + \dfrac{3}{2}\sqrt{\dfrac{R_1(a)-1}{R_1(a)}}\right)da & z \geqslant h_s. \end{cases} \tag{B.30}$$

$$D(z) = \int_0^{(z-h_s)/\varepsilon^\kappa} \frac{S_1(a)^{1-n}}{n} \times \begin{cases} \left(\dfrac{n}{n+2R_1(a)} - [1-R_1(a)]^{(1-n)/n} \right) da & z < h_s, \\ \dfrac{n}{n+2R_1(a)} da & z \geqslant h_s. \end{cases} \tag{B.31}$$

Note that the terms associated to the inner solution (3.14) are significant only in the close vicinity of the fake yield surfaces, since the integrals involved in the functions C, T and D rapidly converge to their respective limits $C(0)$, $T(0)$ and $D(0)$ outside of the transition layer.

C. Expressions of $u^{(1)}$ for the alternative constitutive law with Bingham plateau regularization

Here we provide the full analytical expression of the first-order correction for the longitudinal velocity $u^{(1)}$ resulting from the integration of Equations (4.18) and (4.19). Let us denote:

$$u^{(1)} = I_T(x,z,t)\partial_t h + \Big[I_X(x,z,t) + P(x,z,t) \Big] \partial_x h, \tag{C.1}$$

where the terms I_T and I_X relate to the inertial contributions and the term P relates to the pressure contribution. In the sheared layer ($z < h - h_p$) the expressions for these terms are:

$$\begin{aligned} I_T(x,z,t) = \frac{Re\lambda^{-1+2/n}}{(n+1)(n+2)} \Big\{ & -n\left(h-h_p-z\right)^{1+2/n} + (n+2)\left(h-h_p\right)^{1/n}\left(h-h_p-z\right)^{1/n}\left(nh_p+h-z\right) \\ & - \left(h-h_p\right)^{2/n}\left[n(n+3)h_p+2h\right] + \delta^{\frac{1-n}{n}} \frac{n+2}{2n+1}\left(n\left(h-h_p\right)^{\frac{1}{n}+2} - n\left(-h_p+h-z\right)^{\frac{1}{n}+2}\right) \\ & + \delta^{\frac{1-n}{n}} \frac{z}{2n}(n+1)(n+2)(z-2h)\left(h-h_p\right)^{\frac{1}{n}} \Big\} \end{aligned} \tag{C.2}$$

$$\begin{aligned} I_X(x,z,t) = \frac{nRe\lambda^{-1+3/n}}{2(n+1)^2(n+2)(2n+1)} \Big\{ & \left(h-h_p\right)^{1/n}\left(h-h_p-z\right)^{1/n} \times \\ & \times \Big[2(n+2)(2n+1)\left(h-h_p\right)^{1+1/n}\left(h-z+nh_p\right) - \left(h-z-h_p\right)^{1+1/n}\left(n(5+4n)\left(h-h_p\right)+(2+n)z\right)\Big] \\ & - \left(h-h_p\right)^{1+3/n}\Big[(4+5n)h + n\left(9+14n+4n^2\right)h_p\Big] + \frac{\delta^{\frac{1-n}{n}}}{n}(n+1)(n+2)(2n+1)z(z-2h)\left(h-h_p\right)^{\frac{2}{n}+1} \\ & + \delta^{\frac{1-n}{n}} \frac{2(n+1)(n+2)(2n+1)}{n(6n+5)+1}\Big[\left(h_p-h+z\right)^2\left(\left(h_p-h\right)\left(h_p-h+z\right)\right)^{\frac{1}{n}}\left(3nh_p-3hn-z\right) + 3n\left(h-h_p\right)^{\frac{2}{n}+3}\Big] \Big\}, \end{aligned} \tag{C.3}$$

$$P(x,z,t) = \frac{Re\lambda^{-1+1/n}}{(n+1)Fr^2}\left[\left(h-h_p-z\right)^{1/n}\left(h+nh_p-z\right) - \left(h-h_p\right)^{1/n}\left(h+nh_p\right) + \frac{\delta^{\frac{1-n}{n}}(n+1)}{2n} z(z-2h)\right] \tag{C.4}$$

In the pseudo-plug layer ($z > h - h_p$), the expressions are:

$$\begin{aligned} I_T(x,z,t) = \frac{Re\lambda^{-1+2/n}}{(1+n)} \Bigg\{ & -\frac{\left(h-h_p\right)^{2/n}\left[n(n+3)h_p+2h\right]}{n+2} \\ & + \delta^{\frac{1-n}{n}} \frac{\left(h-h_p\right)^{\frac{1}{n}}\left[-2h\left(-hn^2+n\left(2n\left(h_p+z\right)+3z\right)+z\right)+2n^2h_p^2+(n+1)(2n+1)z^2\right]}{2n(2n+1)} \Bigg\} \end{aligned} \tag{C.5}$$

$$I_X(x,z,t) = \frac{Re\left(h-h_p\right)^{1/n}\lambda^{-1+3/n}}{2\left(n+1\right)^2\left(n+2\right)\left(2n+1\right)}\Big\{ \left(h_p-h\right)\left[n\left(h-h_p\right)^{2/n}\left[n\left(2n\left(2n+7\right)+9\right)h_p+h\left(5n+4\right)\right]\right] \\ +\delta^{\frac{1-n}{n}}\frac{\left(n+1\right)\left(n+2\right)\left(h-h_p\right)^{\frac{1}{n}+1}\left[-2h\left(-3hn^2+n\left(6n\left(h_p+z\right)+5z\right)+z\right)+6n^2h_p^2+\left(n(6n+5)+1\right)z^2\right]}{3n+1}\Big\} \tag{C.6}$$

$$P(x,z,t) = \frac{Re\lambda^{-1+1/n}}{\left(n+1\right)Fr^2}\Big\{ -\left(h-h_p\right)^{1/n}\left(nh_p+h\right)+\frac{\delta^{\frac{1-n}{n}}\left(n+1\right)}{2n}z(z-2h)\Big\} \tag{C.7}$$

D. Alternative expansion with asymptotic matching

To derive a consistent asymptotic expansion in the pseudo-plug layer in the frame of the alternative constitutive law, let us assume that the derivative $\partial_z u$ in this layer is of $O(\varepsilon^\beta)$ with $\beta > 0$. Hence, for $z > h - h_p$, the expansion of the longitudinal velocity reads

$$u(x,z,t) = u^{(0)}_{\rm PP}(x,t) + \varepsilon u^{(1)}_{\rm PP}(x,t) + \varepsilon^\beta u^{**}_{\rm PP}(x,z,t) + \dots \tag{D.1}$$

where $u^{(0)}_{\rm PP}(x,t)$ and $u^{(1)}_{\rm PP}(x,t)$ are given by Equations (4.16) and (4.17). The term $u^{**}_{\rm PP}(x,z,t)$ is an additional correction accounting for the small shear expected in the pseudo-plug layer if the flow is not at equilibrium. The constitutive law (2.16) then yields

$$\varepsilon\tau^{\upsilon(1)}_{xz\rm PP} = \frac{1}{Bi}\frac{\varepsilon^\beta\partial_z u^{**}_{\rm PP}}{\left|\varepsilon^{2\beta}\left(\partial_z u^{**}_{\rm PP}\right)^2+4\varepsilon^2\left(\partial_x u^{(0)}_{\rm PP}\right)^2\right|^{\frac{1-n}{2}}}. \tag{D.2}$$

The value of β is chosen such that both sides of equation (D.2) are of the same order, namely $O(\varepsilon)$. In this paper, we consider only the case $n < 1$. If $\beta \leqslant 1$, the right-hand side of (D.2) is of $O(\varepsilon^{n\beta})$, thus larger than $O(\varepsilon)$. If $\beta > 1$, the right-hand side of (D.2) is of $O(\varepsilon^{\beta+n-1})$, and the choice $\beta = 2-n$ allows us to recover a contribution of order $O(\varepsilon)$. For this value of β, equation (D.2) reduces to

$$\varepsilon\tau^{\upsilon(1)}_{xz\rm PP} = \frac{\varepsilon}{Bi}\left|2\partial_x u^{(0)}_{\rm PP}\right|^{n-1}\partial_z u^{**}_{\rm PP} + O(\varepsilon^{3-2n}). \tag{D.3}$$

Hence, it is observed that the derivative $\partial_z u$ in the pseudo-plug is of $O(\varepsilon^{2-n})$. Accordingly, the solutions (4.16)–(4.17) without shear in the pseudo-plug layer are consistent up to $O(\varepsilon)$.

The solution of (D.3) should be asymptotically matched with (4.16) in the sheared layer by introducing a transition layer, similar as in Appendix B. Let us consider a layer of $O(\varepsilon^n)$ thickness close to the pseudo-plug by introducing the variable $\xi = (h-h_p-z)/\varepsilon^n$. This transition layer formally collapses into the fake-yield surface as $\varepsilon \to 0$. This means that the leading-order solution, which is formally found for $\varepsilon \to 0$, is not modified. In particular, the expression of $u^{(0)}$ already obtained is valid everywhere. We have therefore $\partial_z u^{(0)} = 0$ for $\xi < 0$ (in the pseudo-plug layer) and $\partial_z u^{(0)} = \lambda^{1/n}(h-h_p-z)^{1/n} = \varepsilon\lambda^{1/n}\xi^{1/n}$ for $\xi > 0$. In the transition layer, ξ is of $O(1)$, while in the sheared layer, outside the transition layer, ξ is of $O(\varepsilon^{-n})$.

If we consider the small corrections to the leading-order solution, we notice that, in the transition layer, the term $\partial_z u^{(0)}$ is of the same order of magnitude $O(\varepsilon)$ as the term $\partial_x u^{(0)}$, whereas in the sheared layer, outside the transition layer, $\partial_z u^{(0)}$ is of $O(1)$ and therefore of a greater order of magnitude than $\partial_x u^{(0)}$. This leads to specific corrective terms in the transition layer that are absent outside it. The expansion of $\partial_z u$ in the sheared layer outside the transition layer, can be written up to $O(\varepsilon)$ as $\partial_z u = \partial_z u^{(0)} + \varepsilon\partial_z u^{(1)}$. In the transition layer, two extra terms are needed, and this expansion can be written

$$\partial_z u = \partial_z u^{(0)} + \varepsilon\partial_z u^{(1)} + \varepsilon\partial_z u^{*} + \varepsilon^{2-n}\partial_z u^{**} \tag{D.4}$$

or

$$\partial_z u = \varepsilon \partial_z u^{(0)}_{\mathrm{TL}} + \varepsilon^{2-n} \partial_z u^{(1)}_{\mathrm{TL}} + \varepsilon \partial_z u^{*} + \varepsilon^{2-n} \partial_z u^{**} \tag{D.5}$$

since, in this layer, $\partial_z u^{(0)} = \varepsilon \lambda^{1/n} \xi^{1/n} = \varepsilon \partial_z u^{(0)}_{\mathrm{TL}}$ and

$$\varepsilon \partial_z u^{(1)} = \varepsilon^{2-n} \frac{Bi}{n} (\lambda \xi)^{-1+1/n} \tau^{v(1)}_{xz} = \varepsilon^{2-n} \partial_z u^{(1)}_{\mathrm{TL}}. \tag{D.6}$$

Substituting the expression (D.5) into the constitutive law in the transition layer leads to

$$\begin{aligned} \frac{\lambda}{Bi} \varepsilon^n \xi + \varepsilon \tau^{v(1)}_{xz} = \frac{\varepsilon^n}{Bi} & \frac{\partial_z u^{(0)}_{\mathrm{TL}} + \partial_z u^{*}}{\left| \left(\partial_z u^{(0)}_{\mathrm{TL}} + \partial_z u^{*} \right)^2 + 4 \left(\partial_x u^{(0)} \right)^2 \right|^{\frac{1-n}{2}}} \\ + \frac{\varepsilon}{Bi} & \left\{ \frac{\partial_z u^{(1)}_{\mathrm{TL}} + \partial_z u^{**}}{\left[\left(\partial_z u^{(0)}_{\mathrm{TL}} + \partial_z u^{*} \right)^2 + 4 \left(\partial_x u^{(0)} \right)^2 \right]^{\frac{1-n}{2}}} + \frac{(n-1) \left(\partial_z u^{(0)}_{\mathrm{TL}} + \partial_z u^{*} \right)^2 \left(\partial_z u^{(1)}_{\mathrm{TL}} + \partial_z u^{**} \right)}{\left[\left(\partial_z u^{(0)}_{\mathrm{TL}} + \partial_z u^{*} \right)^2 + 4 \left(\partial_x u^{(0)} \right)^2 \right]^{\frac{3-n}{2}}} \right\} + O(\varepsilon^{2-n}) \end{aligned} \tag{D.7}$$

Note that, in the transition layer, $\partial_x u^{(0)} = \lambda^{1/n} \left(h - h_p \right)^{1/n} \partial_x h + O(\varepsilon)$. It follows that the term $\partial_z u^{*}$ can be found numerically by solving the equation

$$\lambda \xi = \frac{\lambda^{1/n} \xi^{1/n} + \partial_z u^{*}}{\left| \left(\lambda^{1/n} \xi^{1/n} + \partial_z u^{*} \right)^2 + 4 \left(\lambda^{1/n} \left(h - h_p \right)^{1/n} \partial_x h \right)^2 \right|^{\frac{1-n}{2}}} \tag{D.8}$$

If $\partial_x h = 0$ then $\partial_x u^{(0)} = 0$, which implies $\partial_z u^{*} = 0$. This shows clearly that $\partial_z u^{*} = 0$ is a first-order correction, which appears only in variable flows. The term $\partial_z u^{*}$ can be seen as a compensation at the highest order of magnitude ($O(\varepsilon^n)$) of the term $\partial_x u^{(0)}$ in the transition layer.

The term $\partial_z u^{**}$ can then be found by the numerical resolution of the equation

$$Bi \tau^{v(1)}_{xz} = \frac{\partial_z u^{(1)}_{\mathrm{TL}} + \partial_z u^{**}}{\left[\left(\partial_z u^{(0)}_{\mathrm{TL}} + \partial_z u^{*} \right)^2 + 4 \left(\partial_x u^{(0)} \right)^2 \right]^{\frac{1-n}{2}}} + \frac{(n-1) \left(\partial_z u^{(0)}_{\mathrm{TL}} + \partial_z u^{*} \right)^2 \left(\partial_z u^{(1)}_{\mathrm{TL}} + \partial_z u^{**} \right)}{\left[\left(\partial_z u^{(0)}_{\mathrm{TL}} + \partial_z u^{*} \right)^2 + 4 \left(\partial_x u^{(0)} \right)^2 \right]^{\frac{3-n}{2}}} \tag{D.9}$$

At the boundary of the pseudo-plug layer ($\xi = 0$), the resolution of Equation (D.8) yields $\partial_z u^{*} = 0$. Then, at the fake-yield surface, Equation (D.9) reduces to

$$\tau^{v(1)}_{xz} = \frac{\partial_z u^{**}}{Bi} \left[2 \partial_x u^{(0)} \right]^{n-1} \tag{D.10}$$

which coincides with Equation (D.3). This ensures the matching of the solution in the transition layer with the solution in the pseudo-plug layer. When $\xi = O(\varepsilon^{-n})$ (or $\xi \to \infty$), $\partial_z u^{*}$ and $\partial_z u^{**}$ become asymptotically negligible, which ensures the asymptotic matching of the solution in the transition layer with the solution in the sheared layer outside the transition layer.

The terms u^{*} and u^{**} can be found by integrating $\partial_z u^{*}$ and $\partial_z u^{**}$, respectively, over the transition layer. Since the thickness of this layer is of $O(\varepsilon^n)$, the order of magnitude of the terms in u^{*} and u^{**} in the expansion of u are $O(\varepsilon^{1+n})$ and $O(\varepsilon^2)$ respectively. This implies that these terms do not modify the velocity expansion up to $O(\varepsilon)$. Hence, shear effects in the pseudo-plug, and the corresponding terms in the velocity that ensure an asymptotic matching, appear at an order of magnitude smaller than $O(\varepsilon)$. Note also that the introduction of the transition layer does not affect the

expression for the shear stress $\tau_{xz}^{v(1)}$, because its calculation is based on the derivatives of $u^{(0)}$ that are valid everywhere, including the transition layer.

For computing smooth velocity profiles, it is thus possible to numerically integrate the expansion (D.5) with the boundary condition at the bottom, and then to connect the result with the solution in the pseudo-plug (D.1). Instead, we propose another method to compute the velocity profiles, which formally alleviates the need to introduce a transition layer. Namely, in the sheared layer we keep the terms $\partial_z u^*$ and $\partial_z u^{**}$ in the denominator in the constitutive law and return to the variable z:

$$\frac{\lambda}{Bi}\left(h-z-h_p\right)+\varepsilon\tau_{xz}^{v(1)}=\frac{1}{Bi}\frac{\partial_z u^{(0)}+\varepsilon\partial_z u^*+\varepsilon\partial_z u^{(1)}+\varepsilon^{2-n}\partial_z u^{**}}{\left|\left(\partial_z u^{(0)}+\varepsilon\partial_z u^*+\varepsilon\partial_z u^{(1)}+\varepsilon^{2-n}\partial_z u^{**}\right)^2+4\varepsilon^2\left(\partial_x u^{(0)}\right)^2\right|^{\frac{1-n}{2}}}. \tag{D.11}$$

As already mentioned, the terms $\varepsilon\partial_z u^*$ and $\varepsilon^{2-n}\partial_z u^{**}$ are important only close to the fake yield-surface, while these terms are asymptotically negligible close to the bottom. Note also that the term $\partial_x u^{(0)}$ vanishes at the bottom. Equation (D.11) can be solved by considering the sum $\varepsilon\partial_z u^*+\varepsilon^{2-n}\partial_z u^{**}$ as a single unknown variable, while all terms in the right-hand side, both in the numerator and in the denominator, can be consistently kept. In the pseudo-plug, to have a continuous transition from the sheared zone, we should then consider equation (D.2) that keeps the small term $\varepsilon^{2-2n}\left(\partial_z u_{\mathrm{PP}}^{**}\right)^2$ in the denominator:

$$\tau_{xz\mathrm{PP}}^{v(1)}=\frac{1}{Bi}\frac{\partial_z u_{\mathrm{PP}}^{**}}{\left|\varepsilon^{2-2n}\left(\partial_z u_{\mathrm{PP}}^{**}\right)^2+4\left(\partial_x u_{\mathrm{PP}}^{(0)}\right)^2\right|^{\frac{1-n}{2}}}. \tag{D.12}$$

The solution $\varepsilon\partial_z u^*+\varepsilon^{2-n}\partial_z u^{**}$ of the equation (D.11) matches exactly the solution $\varepsilon^{2-n}\partial_z u_{\mathrm{PP}}^{**}$ of (D.12). Keeping all terms in the denominators, both in (D.11) and (D.12), ensures an exact, and not just an asymptotic, connection with the solution in the pseudo-plug, thus better representing the shear near the surge tip, which lies outside the validity domain of the asymptotic developments. Indeed, since the term $\partial_x u_{\mathrm{PP}}^{(0)}$ is zero at $h=h_p$, the term $\varepsilon^{2-2n}\left(\partial_z u_{\mathrm{PP}}^{**}\right)^2$ becomes dominant when $h\to h_p$.

As an example, the velocity profiles obtained by the numerical solution of (4.6), (4.7), (4.16), (4.17), (D.11) and (D.12) are compared to experiments HB3 and HB13 in Figs. 5 and 6. As clear from the figures, the profiles involving the terms u^*, u^{**} and u_{PP}^{**} are in good agreement with the experimental data, even close to the tip of the surges. In particular, the shear rate at intermediate distances from the tip ($x\approx 4$, typically) is not overestimated, as it was the case with the expansions obtained from the classical formulation of the Herschel-Bulkley rheology and asymptotic matching (see Figs. 3-4). For comparison, the profiles obtained from the fully analytical expansion obtained by regularization of the viscous stress tensor at $O(\varepsilon)$ (see Appendix C) are also plotted in Figs. 5 and 6 (dashed red curves). In both cases, a specific value of the regularization parameter δ can be found such that a perfect agreement is obtained with the "full" profiles involving the terms u^*, u^{**} and u_{PP}^{**}. This shows that the contribution provided by the terms in δ in Eqs. (C.1)-(C.7) can be considered as a good approximation of the matching terms u^*, u^{**} and u_{PP}^{**}.

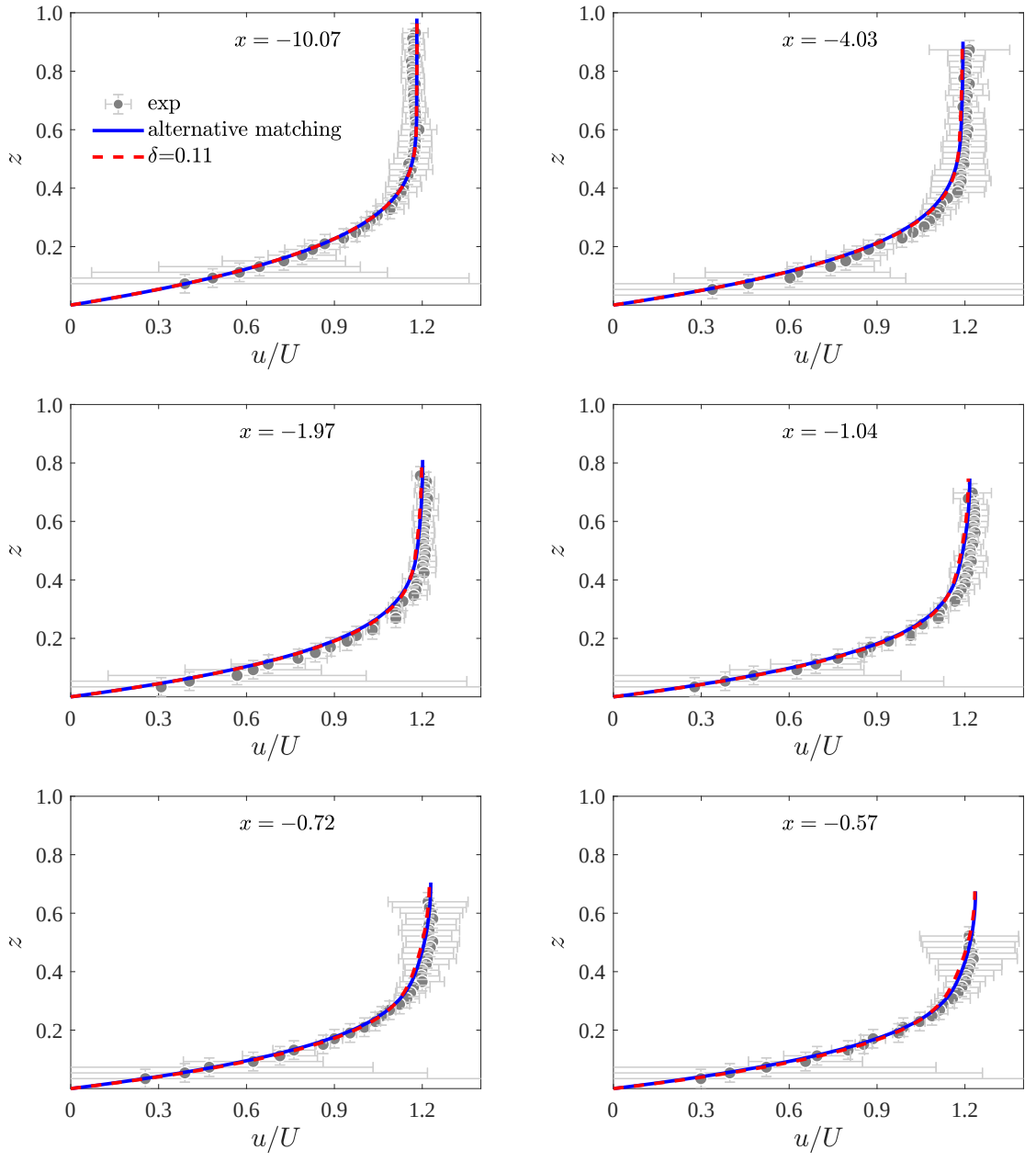

Figure 5: Experimental-theoretical comparison for experiment HB3 (see Table 1): non-dimensional profiles of longitudinal velocity u normalized by the depth-averaged velocity U for six values of the distance from the tip x. Gray dots correspond to experimental measurements with associated error bars, the blue curves correspond to the profiles involving the matching terms u^*, u^{**} and u^{**}_{PP} (see text), and the dashed red curves correspond to the profiles obtained from the regularized expansion with $\delta = 0.11$.

References

[1] M. de Saint-Venant, Théorie du mouvement non permanent des eaux, avec application aux crues des rivières et à l'introduction de marées dans leurs lits, C. R. Acad. Sci. Paris 73 (1871) 147–154 and 237–240.
[2] G. Whitham, Linear and nonlinear waves, New York, Wiley-Interscience, 1974.
[3] S. Kalliadasis, C. Ruyer-Quil, B. Scheid, M. G. Velarde, Falling liquid films, volume 176, Springer Science & Business Media, 2012.
[4] D. Benney, Long waves on liquid films, Journal of mathematics and physics 45 (1966) 150–155.

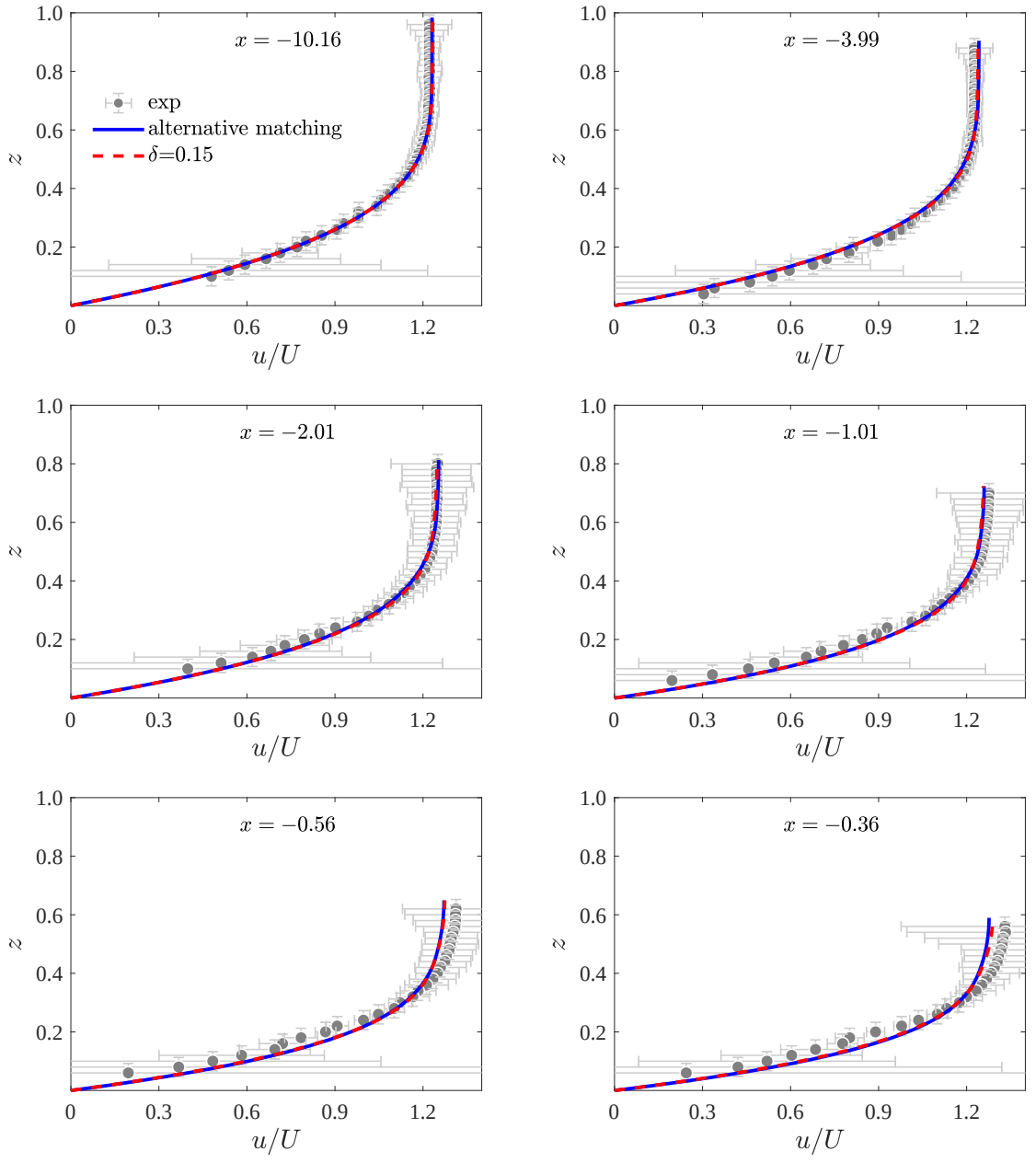

Figure 6: Experimental-theoretical comparison for experiment HB13 (see Table 1): same legend as Fig. 5. Profiles computed from the regularized expansion correspond here to $\delta = 0.15$.

[5] B. Hunt, Newtonian fluid mechanics treatment of debris flows and avalanches, Journal of Hydraulic Engineering 120 (1994) 1350–1363.

[6] H. E. Huppert, Gravity currents: a personal perspective., Journal of Fluid Mechanics 554 (2006) 299–322.

[7] C. Ruyer-Quil, P. Manneville, Modeling film flows down inclined planes, The European Physical Journal B-Condensed Matter and Complex Systems 6 (1998) 277–292.

[8] C. Ancey, Plasticity and geophysical flows: a review, Journal of Non-Newtonian Fluid Mechanics 142 (2007) 4–35.

[9] P. Noble, J.-P. Vila, Thin power-law film flow down an inclined plane: consistent shallow-water models and stability under large-scale perturbations, Journal of Fluid Mechanics 735 (2013) 29–60.

[10] A. Chesnokov, Formation and evolution of roll waves in a shallow free surface flow of a power-law fluid down an inclined plane, Wave Motion 106 (2021) 102799.

[11] C. Ruyer-Quil, P. Manneville, Improved modeling of flows down inclined planes, The European Physical Journal B-Condensed Matter and Complex Systems 15 (2000) 357–369.
[12] R. Usha, B. Uma, Modeling of stationary waves on a thin viscous film down an inclined plane at high reynolds numbers and moderate weber numbers using energy integral method, Physics of Fluids 16 (2004) 2679–2696.
[13] G. L. Richard, S. L. Gavrilyuk, A new model of roll waves: comparison with brock's experiments, Journal of Fluid Mechanics 698 (2012) 374–405.
[14] G. Richard, C. Ruyer-Quil, J.-P. Vila, A three-equation model for thin films down an inclined plane, Journal of Fluid Mechanics 804 (2016) 162–200.
[15] C. on Ng, C. C. Mei, Roll waves on a shallow layer of mud modelled as a power-law fluid, Journal of Fluid Mechanics 263 (1994) 151–184. doi:10.1017/S0022112094004064.
[16] N. Balmforth, J. Liu, Roll waves in mud, Journal of Fluid Mechanics 519 (2004) 33–54.
[17] C. Ancey, S. Cochard, The dam-break problem for herschel–bulkley viscoplastic fluids down steep flumes, Journal of Non-Newtonian Fluid Mechanics 158 (2009) 18–35.
[18] E. D. Fernández-Nieto, P. Noble, J.-P. Vila, Shallow water equations for non-newtonian fluids, Journal of Non-Newtonian Fluid Mechanics 165 (2010) 712–732.
[19] D. Denisenko, G. Richard, G. Chambon, A consistent three-equation shallow-flow model for bingham fluids, Journal of Non-Newtonian Fluid Mechanics 321 (2023) 4–35.
[20] N. J. Balmforth, I. A. Frigaard, G. Ovarlez, Yielding to stress: recent developments in viscoplastic fluid mechanics, Annual review of fluid mechanics 46 (2014) 121–146.
[21] C. Ruyer-Quil, S. Chakraborty, B. S. Dandapat, Wavy regime of a power-law film flow, Journal of Fluid Mechanics 692 (2012) 220–256. doi:10.1017/jfm.2011.508.
[22] M. Boutounet, J. Monnier, J.-P. Vila, Multi-regime shallow free surface laminar flow models for quasi-newtonian fluids, European Journal of Mechanics-B/Fluids 55 (2016) 182–206.
[23] P. Coussot, Steady, laminar, flow of concentrated mud suspensions in open channel, Journal of Hydraulic Research 32 (1994) 535–559.
[24] G. Chambon, A. Ghemmour, D. Laigle, Gravity-driven surges of a viscoplastic fluid: an experimental study, Journal of Non-Newtonian Fluid Mechanics 158 (2009) 54–62.
[25] N. Balmforth, R. Craster, A consistent thin-layer theory for bingham plastics, Journal of Non-Newtonian Fluid Mechanics 84 (1999) 65–81.
[26] G. Chambon, P. Freydier, M. Naaim, J.-P. Vila, Asymptotic expansion of the velocity field within the front of viscoplastic surges: comparison with experiments, Journal of Fluid Mechanics 884 (2020) A43.
[27] P. Coussot, Yield stress fluid flow: A review of experimental data, Journal of Non-Newtonian Fluid Mechanics 211 (2014) 31–49.
[28] K. v. Hohenemser, W. Prager, Über die ansätze der mechanik isotroper kontinua, ZAMM-Journal of Applied Mathematics and Mechanics/Zeitschrift für Angewandte Mathematik und Mechanik 12 (1932) 216–226.
[29] J. G. Oldroyd, A rational formulation of the equations of plastic flow for a bingham solid, in: Mathematical Proceedings of the Cambridge Philosophical Society, volume 43, Cambridge University Press, 1947, pp. 100–105.
[30] I. Frigaard, C. Nouar, On the usage of viscosity regularisation methods for visco-plastic fluid flow computation, Journal of Non-Newtonian Fluid Mechanics 127 (2005) 1–26.
[31] P. Freydier, G. Chambon, M. Naaim, Experimental characterization of velocity fields within the front of viscoplastic surges down an incline, Journal of Non-Newtonian Fluid Mechanics 240 (2017) 56–69. doi:10.1016/j.jnnfm.2017.01.002.
[32] L. P. A, Matched asymptotic expansions: ideas and technique, volume 76, New York: Springer, 1988.